The interplay of epigenetics and metabolism in Alzheimer's disease

Larissa Traxler, M.Sc.

Marshall Plan Scholarship 2019/2020
25.09.2019 – 24.01.2020
University of Colorado, Anschutz Medical Center, Denver
Salk Institute of Biological Studies, San Diego

Supervisor home university:
Asst.Prof. Jerome Mertens
University of Innsbruck, Neural Aging Lab

Supervisor guest university:
Asst. Prof. Angelo D'Alessandro
University of Colorado, Institute of Biochemistry and Molecular Genetics

Prof. Fred. H. Gage
Salk Institute, Laboratory of Genetics

Table of Contents

The interplay of epigenetics and metabolism in Alzheimer's disease

Larissa Traxler[1], Fred H. Gage[2,] Angelo D'Alessandro[3], Jerome Mertens[1]

[1]Institute of Molecular Biology, Leopold Franzens University, Innsbruck, AT
[2]Laboratory of Genetics, Salk Institute of Biological Sciences, San Diego, CA
[3]Institute of Biochemistry and Molecular Genetics, Anschutz Medical Campus, Denver, CO, USA

Abstract
Old age is the most significant risk factor for several diseases, including diabetes, cancer, and a majority of dementias including Alzheimer's disease (AD). A dominating research focus in the AD field has been the characterization of potentially toxic protein oligomers and aggregates. Based on genetic models for the rare familial forms of the disease, a prevailing view that encompasses protein toxicity followed by cell autonomous and inflammation-related neuronal cell death has been established. However, over one-hundred failed clinical trials in the past twenty years were based on this hypothesis, fostering skepticism about the hypotheses and model systems of AD. Due to the inaccessibility of live human brain tissue, direct conversion of patient fibroblasts into induced neurons (iNs) offers a path towards the next generation of disease models. As opposed to rejuvenated induced pluripotent stem cell (iPSC)-derived neurons, direct iN conversion yields neurons with preserved signatures of epigenetic and functional aging. We previously detected AD-specific changes in age-equivalent iNs from AD patients, which were absent in isogenic but rejuvenated iPSC-derived neurons, and that revealed aberrant activation of signaling pathways and a hypo-mature state of AD iNs. Comparison of iNs from 10 AD patients and 10 non-demented controls revealed a metabolic energy crisis in AD iNs, characterized by decreased ATP/ADP levels and increased NAD consumption +; in the absence of a dysfunctional mitochondrial respiration. Paired mass-spectrometry-based metabolomics and transcriptomics revealed a global metabolic transformation of AD iNs towards increased glycolysis, serine biosynthesis, and fatty acid synthesis, which correlates with the hypo-mature neuronal state and increased competence for neuronal apoptosis. Notably, similar metabolic events are a well-known hallmark of cancer, where aberrant aerobic glycolytic activity is known as the Warburg effect. Interestingly, Warburg-related changes and metabolites have been postulated to drive cellular de-differentiation and transformation. Here, we treat AD and control iNs with compounds used in the cancer field to revert the metabolic switch and could see metabolic changes upon treatment. ACLY inhibitor could additionally close the gap between metabolism and epigenetics by decreasing histone acetylation levels. We thus conclude that an age-dependent but AD-specific metabolic switch in neurons might ultimately lead to a neuronal identity crisis that is accompanied by increased cellular vulnerability and impaired functionality, which could be reverted by compounds used in the cancer field.

Abbreviations:
AD – Alzheimer's disease; fAD - familial/early-onset AD; sAD - sporadic/late-onset AD; Aβ - β-amyloid; iPSCs – induced pluripotent stem cells; DCA – dichloroacetate; 2DG - 2-deoxyglucose; ACLY - ATP citrate lyase; ACSS2 - acetyl-CoA synthetase 2; PKM2 - pyruvate kinase muscle isoform 2, HAT – histone acyl transferase; HDAC – histone deacetylase;

Introduction

Alzheimer's disease (AD) is one of the biggest challenges for our health system, as it affects more than 50 million people worldwide without a cure in sight (1). Alzheimer patients develop severe dementia and become unable to perform the simplest every-day tasks shortly after developing the first symptoms. It is anticipated that the first changes in the brain occur years before the first symptoms appear, however no early biomarker has been detected to diagnose AD before the first symptoms of cognitive decline. Heterogeneity within the patients and a lack of understanding of the origins of the disease, make it sheerly impossible to find pathways to target as an early treatment of Alzheimer's.

Since the first description of AD by Alois Alzheimer in 1906, it was believed that the accumulation of a protein called β-amyloid (Aβ) is the trigger of the disease, which was thereafter thoroughly studied in transgenic animal models carrying known mutations of AD patients (2). The amyloid cascade hypothesis, which is still the most widespread hypothesis in AD research and diagnosis, has been increasingly rejected in recent years, as only 2-5 % of all AD patients carry a mutation in the presenilin or amyloid precursor protein gene, resulting in the early-onset or familial form of AD (fAD). The majority of all AD cases are so-called sporadic (sAD), and are based on a combination of genetic and environmental risk factors, with the biggest risk factor being age (3). Genes involved in the development of fAD are no risk factors for sAD, and additionally novel therapies developed to remove Aβ -plaques from the AD brain, showed no effect on the patients' cognitive state (4). In the last years, various 'omics'-technologies gave rise to new insights into changes occurring in fAD besides β-amyloid misprocessing, opening up new avenues for AD research and drug development (5,6).

Most of these studies, however, were carried out in transgenic animal models or induced pluripotent stem cells (iPSCs) carrying the fAD mutations. The inaccessibility of live human brain tissue and the lack of animal models for the non-genetic variant left sporadic AD widely unexplored. Post-mortem brain tissue has been widely used to study AD, however, the heterogeneity of samples due to post-mortem interval, the inability to manipulate the tissue, e.g. for drug treatment, and getting the tissue at the end-stage of the disease pose huge drawbacks of using post-mortem tissue. With the emergence of iPSCs, neurological diseases could first be studied in living human cells, albeit lacking the aging factor, making it challenging to model age-associated diseases like sAD, even though they are a great model for studying fAD (7–10).

In this study we exploit a new model system that directly converts patient-derived fibroblasts into induced neurons (iNs) by an inducible overexpression of two transcription factors: Ascl1 and Ngn2. With the help of small molecules, supporting the conversion to the neuronal fate, fibroblasts convert to iNs within three weeks (9). This approach results in mainly glutamatergic neurons, which, unlike iPSC-derived neurons, maintain age-associated transcriptomic, epigenetic as well as metabolic features (9,11–13). It is suggested that iNs, since they maintain features of aging, may also maintain environmentally-induced changes to the epigenome that could be disease relevant. Since sAD is a disease that is not only affected by several risk genes, but mainly by environmental factors, iNs pose a great human in-vitro model to study sAD.

Multiple lines of evidence suggest that a dysfunctional cellular metabolic homeostasis plays a major role in aging and age-associated diseases like AD (14,15). Despite its small size, the brain is known to be the biggest consumer of energy in the body and relies heavily on the more effective oxidative phosphorylation rather than glycolysis to produce the energy required to maintain neuronal activity (16). A metabolic switch from aerobic glycolysis in

neural progenitor cells to oxidative phosphorylation in post-mitotic neurons is essential for successful differentiation. Cells that fail to perform this metabolic switch, undergo apoptosis, highlighting the importance of oxidative phosphorylation for post-mitotic neurons (12).

In contrast to cellular differentiation, a reverse metabolic switch from oxidative phosphorylation to aerobic glycolysis, called the Warburg effect, was observed in malignant transformation in cancer where post-mitotic somatic cells de-differentiate to highly proliferative cancer cells, further supporting the role of metabolism in the process of cellular differentiation (17–19). Even though AD and cancer appear to be very different diseases, resulting in either extended growth or exacerbated cell death, first studies have shown that, similar to cancer cells, AD neurons carrying presenilin mutations present a de-differentiated phenotype and signs of a re-entry into the cell cycle, resulting in dysfunctional neurons (20). Further, meta-analyses revealed a direct co-morbidity of AD with the brain tumor glioblastoma, both showing a dysregulation of pathways involved in the metabolic switch and neural differentiation (21). As mature post-mitotic neurons are programmed to prevent apoptosis in order to maintain the neural network and integrity in the brain, a de-differentiation and supposedly a cell cycle re-entry are required to prime neurons for cell death in AD brains (22–24). Recently, we could show that AD iNs are transcriptionally in a 'hypo-mature' state, which is functionally supported by a decrease of synapses compared to healthy old control iNs (Mertens, et al., in review). We hypothesize, that this hypo-mature state of AD iNs results in, or is caused by, a metabolic dysfunction similar to the Warburg effect in cancer, however resulting in increased apoptotic competence rather than proliferation.

Metabolic analysis of post-mortem brain and patient-derived fibroblasts further support the role of metabolism in the pathophysiology of the AD (14,25,26). As it has been suggested the metabolism plays a role at the very first steps of differentiation, the metabolic switch may be present at very early stages of the disease, rendering metabolism a promising drug target at early stages of the disease (27). Targeting the metabolic switch is already a well-studied treatment strategy in cancer, with first compounds already in clinical trials, providing several established compounds for AD research (28,29).

Preliminary data of directly converted iNs comparing sporadic AD patients to healthy old control donors revealed a metabolic switch from oxidative phosphorylation to increased aerobic glycolysis on transcriptomic and metabolic level. This metabolic switch came along with a decreased number of synapses and increased chromatin openness, suggesting a hypo-mature phenotype of AD iNs (Mertens et al., in revision).

In this study we investigate the effect of metabolism on neuronal differentiation and the AD pathology in patient-derived induced neurons. Recently, treatment with NR, a NAD^+ precursor, has been shown to increase neurogenesis and ameliorate the AD phenotype on behavioral level in a mouse model of AD, the molecular background for this effect, however, is unknown (30). Based on these findings, we hypothesize that targeting the metabolism could be a plausible target to treat AD in early stages. Thus, we are going to test the ability of NR to revert the metabolic switch in AD iNs and investigate its effects at molecular level in the cells. NR is proposed to not only target cellular metabolism, but also reduce reactive oxygen species (ROS) and act as a co-factor for enzymes like sirtuins or PARP, resulting in an increase of general cellular fitness resulting in longevity (31–33).

In order to further evaluate the effects of specific metabolic changes on the AD phenotype, we also treated AD iNs with additional compounds targeting cellular metabolism. Shikonin inhibits the dimeric form of pyruvate kinase muscle isoform 2 (PKM2), which is the

inactive form of PKM, reverting the slow conversion of phosphoenolpyruvate to pyruvate in PKM2 overexpressing cells. High dimeric PKM2 levels result in an accumulation of glycolytic metabolites and a decreased glucose flux into the TCA cycle, typical for the Warburg effect in cancer. Further, dimeric PKM2 promotes the conversion of pyruvate into lactate by interacting with HIF1 α, Histone 3, and JMJD5 in the nucleus to increase transcription of LDHA and other glycolytic genes (34,35). Small molecules like Shikonin are able to induce tetramerization of PKM2, activating its kinase function to increase pyruvate production and further preventing its entry into the nucleus (34,35).

In a third approach, we targeted the assumed hyperacetylation in AD iNs by preventing the formation of AcetylCoA in the cytoplasm or nucleus. AcetylCoA can be derived from citrate, which is generated in the mitochondria to be exported to the desired location. Since AcetylCoA is not able to cross any membranes, it is dependent on the derivation from citrate by ATP citrate lyase (ACLY) or from acetate by acetyl-CoA synthetase 2 (ACSS2) (36,37). Increased acetylation, e.g. due to decreased NAD^+ levels, can disturb the interaction of proteins and open up chromatin, making it susceptible to DNA damage. Inhibition of ACLY or ACSS2 has been suggested as a novel anti-cancer strategy targeting glucose and lipid metabolism and could be a possible target in our AD model (38–41).

Additionally we inhibited glycolysis with 2-deoxyglucose (2DG) and promoted glucose oxidation with dichloroacetate (DCA) (42). These treatment strategies, however, were not further evaluated.

Our findings presented here demonstrate profound effects of ACLY inhibitor and shikonin on the metabolic landscape of AD iNs, decreasing glycolysis and increasing the flux of the TCA cycle. Further, ACLYi closed the gap between metabolism and epigenetics, as it has also shown effects on histone acetylation. Our data suggests that ACLY inhibitor is a promising compound that should be further evaluated in AD iNs, however, a combination of different compounds to target several aspects of metabolism seems to be the best option to ameliorate AD phenotype.

Methods

Cell Culture

Human fibroblasts were obtained from the Alzheimer disease research center (ADRC) and were cultured in DMEM + 15 % fetal bovine serum and transduced with lentiviruses containing Ngn2 and Ascl1. Once confluent, fibroblasts were pool-splitted for direct conversion in NK medium to induced neurons (iNs) (described in detail in (9)). After FACS sorting for PSA-NCAM positive cells, cells were plated on Geltrex coated plates and cultured for 3 days in BrainPhys (StemCell Technologies, #05790). For Mass Spectrometry based analysis, cells were treated for 6 hours with C13-labelled Glucose (Santa Cruz, sc-239643) before pelleting and stored at -80 °C. Treatment with NR (ChromaDex, Niagen lot#40c910-18202-92), Shikonin (Santa Cruz, sc-200391), DCA (Merck, #347795), 2DG (FisherScientific, #10560371), SB204990 (MCE, HY-16450), ACSS2i (Selleckchem, #S8588) was performed in BrainPhys-NK for 3 days.

Apoptosis

100k FACS sorted iNs are seeded on Geltrex coated 96 well plate for imaging (ibidi, #89626). Cells were treated with Staurosporine (MCE, HY-15141) or ABT737 (Tocris, #6835) for 6 hours, before assessing cell viability with AlamarBlue (ThermoFisher Scientific, DAL1025) and subsequent fixation for Cleaved-Caspase3 staining (CellSignaling, #9661).

Seahorse analysis

iNs were FACS sorted and plated at a density of 50.000 cells per well (96 well plate) on seahorse culture plates coated in Polyornithine/Laminin one day prior to assay. Seahorse XP Cell Mito Stress Test was performed according to the protocol provided (Seahorse, Agilent Technologies). Data was normalized to total protein measured by Pierce BCA Protein Assay Kit (ThermoFisher Scientific, #23225).

Lactate measurement

After FACS sorting, 100.000 cells were plated on a Geltrex coated white 96 well plate and treated for 3 days. Supernatant was saved for Lactate assay (Biovision, #K607), which was performed according to the manufacturers protocol.

Histone acetylation

Cells were fixed using 4 % Paraformaldehyde and stained with anti-histone 3 acetylation (Millipore, #06-599), anti-histone 3 (CellSignalling, #14269S) and anti-MAP2 (Abcam, ab5392). Pictures were taken using the EVOS XL Core and analyzed with ImageJ. For analysis, region of interest was set according to DAPI staining and a threshold for MAP2 was set. ROIs with high MAP2 signal were analyzed for histone 3 and histone 3 acetylation.

Semi-quantitative Metabolomics

Cell pellets and supernatant of treated iNs (150.000 FACS sorted cells) were resuspended in Lysis Buffer (50:30:20 MeOH:Acetonitrile(ACN):H_2O, 2 Million cells per mL) or mixed 1:25 in Lysis Buffer, respectively. After vortexing for 30 minutes at 4 °C, proteins were precipitated when centrifuging for 10 minutes at 18.000 x g at 4°C. The supernatant containing metabolites was resolved over the Kinetex C18 column (2.1 x 150 mm, 1.7 µm, Phenomenex) using a Vanquish UHPLC system and analyzed with the high-resolution Q Exactive mass spectrometer (Thermo Scientific) at 35 °C. A volume of 10 µl for pellets and 20 µl for supernatant analysis

was injected for positive and negative ion mode, using a 5 minutes gradient at 450 µl/min from 5% to 95% of ACN/0.1% Formic Acid In Water/0.1% Formic Acid (positive mode) and 95% ACN/5% water/1mM ammonium acetate in 5% ACN/95% water/1mM ammonium acetate (negative mode). Raw files were converted to mzXML file format using Raw converter (43) and technical replicates were used to control technical variablilty. Only metabolites with a coefficient of variation (CV = SD/mean) < 20% were considered for this report. Metabolite assignment to KEGG compounds was performed using MAVEN and normalization to protein content measured with nanodrop was performed with Metaboanalyst.

RedOx & CoA quantification

To run the RedOx and CoA method, extracted metabolites were dried down using a Speed Vac concentrator and resuspended in Lysis Buffer substituted with 15 % Methanol and 5 mM Ammoniumacetate at pH 9. Metabolites were resolved over the Acquity BEH-C18 (CoA) or BEH-Amide (RedOx) columns (2.1 x 150 mm, 1.7 µm, Waters) as described above. A volume of 4 µl was injected to run in positive mode, running a 7 minutes gradient at 450 µl/min.

Acetylome

All steps were performed according to the protocol of the PTMScan® Acetyl-Lysine Motif [Ac-K] Kit (Cell Signaling, #13416). Shortly, one million cells were lysed using a urea lysis buffer and sonication, reduced and alkylated when applying an iodoacetamide solution and digested with LysC over night. Peptides were acidified and purified with 1 % trifluoroacetic acid and provided columns. Acetylated peptides were purified using the antibody beads provided by the kit, followed by a concentration and purification of eluted peptides with C18 StageTips before being run on a nanoUHPLC-high resolution Quadrupole Orbitrap Mass Spectrometer (nanoEasy LC II – Qexactive HF, Thermo Fisher) with Mobile Phase A being 2% ACN/98% H2O/0.1% FA and Mobile Phase B being 98% ACN/2% H2O/0.1 % FA. Raw files were analyzed using Mascot and Proteome Discoverer 2.1 (Thermo Fisher), as extensively described elsewhere.

Results

AD iNs are in an energy crisis despite functional oxidative phosphorylation

Alzheimer disease is characterized by a loss of functional neurons resulting in severe dementia. The cause of the severe cell death and loss of functional synapses in the human brain is still not understood. Due to the inaccessibility of live human brain tissue of patients and the difficulties with modeling sporadic age-associated diseases with animal models or iPSCs, we started to work with direct conversion of patient-derived fibroblasts to neurons (induced neurons, iNs). INs have been shown to resemble many aspects of aging, such as mitochondrial, epigenetic and transcriptomic aging (9,44,45). Recently, we could show that iNs derived from AD patients and age-matched healthy control donors are in a hypo-mature state with aberrant gene expression and increased chromatin openness (Mertens et al., in review). Functional analysis could show that AD iNs have a decreased number of synapses in culture, resembling the first stages of AD, in which the loss of information precedes excessive neuronal cell death (Mertens et al., in review).

Apoptosis is a rare event in mature, differentiated neurons as they are programmed to maintain the integrity of the neuronal network and exhibit so-called anti-apoptotic brakes (22). According to this hypothesis, fully mature neurons are not able to undergo apoptosis under stress, but rather enter a senescent state. To test whether AD iNs are more prone to undergo apoptosis, we treated FACS-sorted iNs derived of 10 healthy old control donors and 8 AD patients (Fig. 1a) with the protein kinase inhibitor Staurosporine and the Bcl-2 inhibitor ABT-737 to induce apoptosis. AD iNs showed increased apoptotic competence as measured by cleaved-caspase 3 positive nuclei after a 6-hour treatment with each compound, which was confirmed by Alamar Blue incubation to measure the number of metabolically active cells as a measure of surviving cell number (Fig. 1b). This suggests that AD iNs are in a more de-differentiated state that enables them to circumvent the anti-apoptotic brake present in fully mature post-mitotic neurons.

Next, we were wondering if AD iNs show signs of a metabolic hypo-mature state. First analysis of their energy state revealed that AD iNs are in an energetic crisis, shown in the decreased ATP/ADP ratio (Fig. 1c). Cytosolic ATP/ADP ratio is an important determinant of preferred glycolysis or oxidative phosphorylation, in which high ATP/ADP ratio suggests high mitochondrial function and decreased glycolysis as present in most post-mitotic cells (46). Mitochondrial dysfunction or hypoxia results in a decreased ATP/ADP ratio, inducing glycolytic activity, a phenotype also observed in the Warburg effect (46). The energetic crisis in AD iNs, however, is not based on a mitochondrial dysfunction as shown in seahorse analysis (Fig. 1d), whereas glycolytic activity and therefore lactate production was increased (Fig. 1e).

These results suggest that Alzheimer's disease shows a metabolic switch similar to the Warburg effect, resulting in increased aerobic glycolysis despite intact mitochondrial function (Fig. 1f).

Metabolic Switch to increased aerobic glycolysis in AD iNs

The Warburg effect is characterized by an accumulation of glycolytic metabolites, presumably due to the dimeric form of PKM2, slowing down the conversion of phosphoenolpyruvate to pyruvate to provide the cell with starting material for biosynthetic processes, like serine, glycine, glutathione, etc. generation (34,35,47). Transcriptomic analysis of our AD cohort revealed a significant upregulation of genes involved in the glycolytic and associated pathways (Fig. 2a). To check if changes observed on RNA level can be translated into protein level, we performed semi-quantitative metabolomics, revealing an accumulation

of certain glycolytic metabolites, glyceraldehyde-3-phosphate being the only glycolytic metabolite being decreased in AD iNs (Fig. 2a,b). As metabolites of the TCA cycle were mainly unaffected in AD, we anticipated that more glucose is processed in AD iNs to increase glycolytic activity with intact TCA cycle function. Analyzing glucose concentrations in the supernatant, we could show that AD iNs increased glucose consumption (Fig. 2c).

Next, we wanted to see if the intact TCA cycle derives carbons from glucose or increases the uptake of other carbon sources, like glutamine. Therefore, we performed glucose flux analysis by treatment with 50% uniformly-labeled U-$^{13}C_6$-glucose and traced heavy isotopologue intermediates of glycolysis and the TCA cycle (Fig. 2d). We could show that significantly less citrate M+2 is produced in AD iNs compared to increased incorporation of glucose derived carbons in lactate (Fig. 2d,e). Interestingly, however, α-ketoglutarate (α-KG) did incorporate far less labelled glucose compared to citrate (Fig. 2f,g), even though when looking at total metabolite abundance, AD iNs have slightly more α-KG/Citrate than age-matched controls (Fig. 2h). This suggest that AD iNs have an increased demand of citrate, which is further supported by elevated ratio if IDH1 to IDH3, two isoforms of the isocitrate dehydrogenase that either convert α-KG to citrate or citrate to α-KG, respectively (Fig. 2i,j). Further, this suggests that α-KG derives carbons from other sources like glutamine. In contrast to iNs, fibroblasts do not show any AD-specific changes on metabolic level, suggesting that this phenotype is neuron-specific.

NR treatment ameliorates the metabolic switch in AD induced neurons

NAD^+ stands out as an important regulator of cellular metabolism and its decline has been shown to play an essential role in aging and age-related diseases (48). Primarily known for its functions as a redox reagent to link glycolysis and TCA cycle to oxidative phosphorylation, it has later been discovered that NAD^+ also acts as a cofactor for PARPs and Sirtuins, controlling DNA repair, activity of a variety of proteins through post-translational modifications, and histone acetylation (49,50). Regulators that play essential roles in the metabolic switch as observed in AD iNs, like PGC-1α or HIF-1α, are targets of NAD^+-dependent sirtuins, emphasizing the role of NAD^+ in mediating the Warburg-like phenotype (50).

To start with, we investigated weather iNs derived from AD patients have lower levels of NAD^+. Transcriptomic data of our AD cohort suggested an increase in NAD^+ biosynthesis in AD iNs, as genes like NAMPT (nicotinamide phosphoribosyltransferase), KMO (Kynurenine 3-monooxygenase), QPRT (quinolinate phosphoribosyltransferase), and NMRK1 (Nicotinamide Riboside Kinase 1) were significantly upregulated. Colorimetric analysis of sorted iNs revealed that, in contrast to increased gene expression of genes related to NAD^+ biosynthesis in AD iNs, decreased amount of free NAD^+ is available in AD neurons (Fig. 3b). This suggests that AD iNs have increased demand for NAD^+ consumption, supporting the hypothesis of an energy crisis.

This data shows a correlation of decreased NAD^+ levels and the metabolic switch to increased aerobic glycolysis. To test this, we treated iNs derived from patient 2800 and from control line 2608 with NR, a NAD^+ precursor that is currently used in preclinical studies to evaluate its effects on aging, longevity and diseases. A treatment period of 3 days was set in this pilot experiment (Fig. 3c). NR is the drug of choice for elevating NAD+ levels in many studies, as it can be taken up orally by patients and can be used as a dietary supplement which is already on the market. Additionally, previous experiments in a mouse model of AD could show that substitution of drinking water with NR for 6 months was enough to ameliorate many of the behavioral AD symptoms, like memory and anxiety (30).

Based on this data, we first evaluated survival of sorted iNs after treatment with NR. Cell count with a Neubauer chamber after harvesting the iNs after the 3 day NR treatment revealed a negative effect of NR on survival rates of AD iNs, in contrast to improved survival in the control iNs (Fig. 3d). Further, NR failed to decrease the ratio of glycolytic metabolites to metabolites of the TCA cycle in AD iNs and even doubled the ratio in control cells (Fig. e). Nevertheless, NR was able to normalize Lactate secretion and glucose consumption to a level comparable to control cells (Fig. 3f). Analyzing glycolytic and TCA metabolites in more detail, we could observe an accumulation of Biphosphoglycerate in AD neurons treated with NR, despite successfully decreasing all other glycolytic metabolites (Fig. 3g). Additionally, the production of Lactate compared to Citrate and the production of Lactate per glucose could be decreased in AD iNs (Fig. 3i). Nevertheless, NR additionally decreased most of the metabolites in the TCA cycle, explaining the increased glycolysis/TCA ratio (Fig. 3h). To check whether the decrease in TCA cycle metabolites derives from decreased production or increased consumption, we treated the cells with C_{13}-glucose for 6 hours to trace labelled carbons derived from glucose during that period. Previous experiments have shown that AD iNs have significantly less labelled citrate M+2 compared to lactate M+3 (Suppl. Fig. 1e). NR treatment slightly increased the citrate M+2/lactate M+3 ratio (Fig. 3j, Suppl. Fig. 1a), suggesting increased glucose utilization for TCA cycle metabolites.

Next we looked into the labelling of carbons in citrate. Citrate derives two carbons from glycolysis, and three carbons through glucose dependent anaplerosis, in which pyruvate is transformed to oxaloacetate. This pathway is increasingly used in malignant transformation, as it contributes to biomass assimilation and cell growth (51). Whereas citrate M+2 was unaffected by NR treatment, it could decrease M+3 (Suppl. Fig. 1c). Additionally, NR was able to increase the M+4 form of citrate, suggesting increased TCA cycle turnover, restoring it to a normal level (Suppl. Fig. 1c). This indicates that TCA cycle metabolites are decreased due to increased consumption and utilization of intermediates. This is further supported by the increased labelled α-KG per citrate ratio (Fig. 3j), as AD iNs have been shown to increase citrate production from α-KG by overexpressing IDH1 resulting in a significantly decreased amount of glucose-derived α-KG (Suppl. Fig. 1f,g).

NR treatment could increase metabolic activity of AD iNs, and further decrease excessive glycolytic activity, normalizing glucose consumption and lactate excretion to a level similar to control cells and improving glucose flux to α-KG.

Inhibiting AcetylCoA production in cytosol and nucleus

The Warburg effect in cancer is not solely characterized by increased aerobic glycolysis, but is a complex dysregulation of metabolic pathways. Fatty acid synthesis (FAS) is highly increased in cancer cells, which was also dysregulated on transcriptomic level in our AD cohort, where enzymes involved in the de-novo FAS from cytosolic acetylCoA were highly enriched in AD iNs (Suppl. Fig. 1h). FAS is dependent on citrate derived from the mitochondria, since acetylCoA itself is impermeable to cellular membranes. Citrate, derived from glucose or other carbon sources, is exported to the cytoplasm where it is converted by the enzyme ACLY to acetylCoA, which is used for FAS. Apart from FAS, cytosolic and nuclear acetylCoA formation by ACLY plays an essential role in protein and histone acetylation, displaying a crucial crosstalk between metabolism and epigenetic regulation. Previous data showed that AD iNs have increased chromatin openness, resulting in a de-differentiated state of AD neurons (Mertens et al., in review). Histone hyperacetylation, amongst others, is able to increase chromatin openness and has been shown to be involved in DNA-repair associated

opening of chromatin, but also plays an essential role in cellular differentiation (27,52). Our data could show an increased acetylation of histone 3 in AD iNs, which has to be further validated by mass-spectrometry-based acetylomics (Suppl. Fig. 1i). The rate limiting enzyme in this step is ACLY, which converts citrate and coenzyme A to acetylCoA and oxaloacetate in the cytosol or nucleus. Inhibition of ALCY has been used to treat a variety of metabolic diseases and has lately gained popularity in the cancer field to inhibit FAS (53,54).

Here, we treated AD iNs with the ACLY inhibitor SB204990 (from heron called SB or ACLYi) that has been shown to decrease FAS in tumor cells (55). ACLYi was able to successfully decrease fatty acid synthesis, as all eight fatty acids detected with our metabolomics method were decreased in the treated cells (Fig. 4a).

Next, we evaluated whether SB has effects on the general metabolic landscape of AD iNs, focusing in glycolysis and the TCA cycle. We could show that ACLYi decreased the glycolysis/TCA ratio, which resulted from a decrease of some of the glycolytic enzymes, but mainly from an increase of TCA cycle intermediates (Fig. 4b,e,f). Lactate excretion into the supernatant, as well as glucose consumption was efficiently decreased in treated AD iNs (Fig. 4c, Suppl. Fig. 1a). Nevertheless, most glucose in ACLY treated AD iNs was used for Lactate production and glucose flux into the TCA cycle was still low, which is shown by the low incorporation of C_{13} into citrate compared to lactate (Fig. 4g). As shown in NR treatment, ACLY inhibition resulted in increased TCA cycle activity (Suppl. Fig. 1c) and could further increase glucose flux from citrate to α-KG, reverting the blockade observed in AD iNs (Fig. 4g), rendering ACLY inhibition a possible mechanism to decrease glucose consumption and increasing glucose-dependent TCA cycle activity.

In a similar approach we inhibited acetylCoA production from external acetate via inhibition of ACSS2. ACSS2 has been shown to play an essential role in histone acetylation and further contributes to the Warburg effect by supplying the tumor cells with additional carbon sources to keep their metabolism upright (36,56,57). ACSS2 inhibition could decrease the glycolysis/TCA ratio in AD iNs and further decreased lactate excretion and glucose consumption to control levels. Nevertheless glycolytic metabolites were still increased compared to control iNs. Lactate/citrate levels suggest that ACSS2 treated cells are still rather glycolytic, however decreasing lactate production compared to untreated AD iNs (Fig. 5e). Strikingly, treated AD iNs dramatically decreased their α-KG/citrate ratio, suggesting that acetate plays an essential role in contributing as a acetyl donor in AD (Fig. 5e). ACSS2 inhibition, despite normalizing some aspects of the metabolic switch, does not improve glucose-dependent α-KG production, but rather decreases the α-KG pool.

Activation of PKM2 reverts most aspects of the metabolic switch

The conversion of phosphoenolpyruvate (PEP) to pyruvate is a rate-limiting step in the glycolytic pathway and is regulated by pyruvate kinase muscle isoform (PKM). PKM exists as two isoforms which are generated by exclusive alternative splicing of exon 9 and exon 10. PKM1, containing exon 9, displays high affinity to PEP and is highly active, whereas PKM2, which expresses exon 10 instead of exon 9, exists as dimer with low affinity to PEP and as tetramer with similar affinities as PKM1 (58,59). Dimeric PKM2 does not exclusively function as a kinase in the glycolytic pathway, but can also enter the nucleus and interact with transcription factors and other regulators, such as STAT3, HIF1α or β-catenin, to activate glycolytic gene transcription (59). Small molecules have been designed to activate PKM2 through tetramerization, preventing its nuclear functions and increasing affinity for PEP.

Transcriptomic analysis of our AD cohort revealed a shift to increased PKM2 expression in AD iNs (Fig. 6a), rendering PKM2 a plausible target for reverting the metabolic switch. Shikonin, as a natural occurring compound, has been shown to specifically inhibit PKM2, resulting in a decreased glycolytic rate, lactate production and glucose consumption in cancer cells (60). Here, we treated AD and control iNs with shikonin with and without the addition of NR (hereafter called shikonin and shikonin+, respectively) for 3 days. Metabolic analysis revealed a substantial decrease of glycolysis/TCA ratio in cells treated with shikonin only, whereas the addition of NR did not show that effect (Fig. 6b). As observed in cancer cells, we could additionally decrease lactate excretion and glucose consumption in both treatment conditions (Fig. 6c). Glycolytic metabolites could be decreased to a similar level as control iNs in both conditions, however shikonin could additionally increase citrate and α-KG levels (Fig. 6e). Glucose flux analysis confirmed that shikonin is able to overcome the IDH blockade, displaying increased labelled α-KG/citrate ratios (Fig. 6f). Shikonin+ increased glucose flux to α-KG and additionally augmented TCA cycle turnover as shown by highly increased citrate M+4 (Fig. 6f, Suppl. Fig. 1c). Activation of PKM2, with or without NR, results in a decrease of glycolysis and increased TCA cycle activity, representing an attractive target to revert the metabolic switch in AD iNs.

Combination of an inhibition of glycolysis and activation of TCA cycle did not show expected results

As a proof of principle, we treated the cells with compounds to inhibit hexokinase-2 (HK2), the first enzyme in the glycolytic pathway with 2-deoxyglucose (2DG) and dichloroacetate (DCA), the inhibitor of pyruvate dehydrogenase kinases (PDKs) resulting in an activation of pyruvate dehydrogenase (PDH) and increased glucose flux into the TCA cycle (61,62). First analysis showed, however, that treatment of control iNs with 2DG and DCA resulted in a drastic increase in glycolysis/TCA ratio, which could be solely attributed to an accumulation of pyruvate in 2DG/DCA treated cells, whereas glycolytic metabolites like glucose-6-phosphate and lactate where highly decreased after treatment. Nevertheless, also TCA cycle intermediates were found to be decreased despite DCA treatment (Suppl. Fig. 1j). Treatment of AD iNs did not show the accumulation of pyruvate, even though TCA cycle intermediates were also decreased (Fig. 7a,c,d). Extracellular lactate and glucose consumption could be decreased as expected (Fig. 7b), whereas glucose flux into the TCA cycle could not be improved (Fig. 7f). This suggests that DCA did not exert its function, resulting in a general decrease of metabolism in the cells. Control cells further accumulated pyruvate, which was not further processed in the TCA cycle.

Correlation of compound-induced changes of Lactate excretion and Histone acetylation

We could show that Alzheimer disease iNs show a metabolic switch to increased glycolysis despite normoxic culture conditions. This phenotype is observed in various cancer types, in which the metabolic switch is supposed to accelerate de-differentiation and malignant transformation (51,63). Previously, we observed that additionally to the metabolic switch, AD iNs show increased chromatin openness as evaluated by ATAC-Seq (Mertens et al., in review), which is characteristic for a de-differentiated phenotype. It has been hypothesized that increased aerobic glycolysis supports de-differentiation by producing acetyl-CoA which serves as an acetyl-donor for protein and histone-acetylation (64). Increased histone acetylation results either from increased histone acyl-transferase (HAT) activity and acetyl-

CoA consumption or decreased activity of histone deacetylases (HDACs), like sirtuins due to the lack of their substrate NAD^+ (65,66).

Targeting metabolism has been an attractive target in cancer therapies, since the metabolic switch is a common dysfunction in a broad range of cancer types (63). Since AD iNs show a similar metabolic phenotype as cancer cells, we tested different compounds developed to revert the metabolic switch and evaluated their effects on their metabolic profile in a pilot study. In the next step, we tested the most promising compounds and combination, which are NR, ACLYi with and without NR, Shikonin with and without NR, and all three compounds together to look at lactate excretion and histone acetylation. In this experiment we were evaluating the interaction of metabolism with epigenetic changes.

As we have shown before, untreated iNs of 4 AD lines show increased lactate excretion and histone acetylation compared to 4 age-matched controls (Fig. 8a,c). Neither of the compounds affected lactate secretion in control cells (Fig. 8a,b), and only a combination of all three compounds decreased histone acetylation in control iNs (Fig. 8c,d). On the other hand, ACLYi and ACLYi in combination with NR successfully decreased lactate secretion into the supernatant and additionally could decrease histone 3 acetylation (Fig. 8). Further, correlating lactate excretion and histone acetylation after treatment could show that the effects are AD specific, as no correlation was observed in control iNs, whereas AD iNs show a significant positive correlation.

Together with the data from the metabolic profile, we hypothesize that ACLYi in combination with NR and shikonin could be an approach to revert the metabolic switch and normalize the epigenetic landscape of AD iNs.

Discussion

A tight regulation of metabolic homeostasis is crucial for maintaining the mature differentiated state in post-mitotic cells. During the differentiation process, cells have to undergo a metabolic switch from glycolysis in stem cells and progenitor cells to oxidative phosphorylation in fully differentiated cells. This metabolic switch is especially important in neurons, which are depleted of their ability to differentiate when glycolysis is artificially overexpressed (12). De-differentiating cells, as observed during iPSC-reprogramming or tumor development, undergo a metabolic switch from oxidative phosphorylation to glycolysis, as described extensively in the cancer field as the Warburg effect (17,67,68). Our study addressed the role of the metabolic switch in Alzheimer's disease and evaluated the utility of certain compounds developed to target the Warburg effect in cancer to treat AD. We could show that AD iNs increase glycolytic activity, despite functional mitochondrial oxidative phosphorylation (Fig. 1). Further, a decreased glucose flux from citrate to α-KG and an increase in IDH1/IDH3 ratio, despite decreased levels of total citrate, suggest increased citrate utilization for other pathways than the TCA cycle, such as FAS or protein/histone acetylation (Suppl. Fig. 1e-h). This was further supported by increased histone acetylation in AD iNS and chromatin openness as assessed by ATAC-Seq (Suppl. Fig. 1i). These result point towards a de-differentiated phenotype of AD iNs, which was underlined by increased apoptosis competence (Fig. 1b) and decreased synapse formation in AD neurons.

In this pilot study, we investigated the effects of NR, a NAD+ precursor, an ACLY or ACSS2 inhibitor, 2DG in combination with DCA, and shikonin, a PKM2 activator, on the metabolic profile of AD and control iNs. Several compounds could decrease the glycolysis/TCA ratio, such as ACLYi, ACSS2i and Shikonin. Despite expected for shikonin, since it's targeting the enzyme deciding over the glycolytic or TCA cycle fate of pyruvate, ACLYi surprisingly had

severe effects on glycolytic activity of the cells, as shown by highly decreased glucose consumption and lactate excretion. This suggests, that the metabolic switch aids to produce acetylCoA via ACLY, forcing the cell to increase glycolysis and glutaminolysis. In contrast to that findings, ACSS2 inhibition did not result in an increase in glucose consumption but rather decreased glucose consumption, suggesting that the lack of acetate metabolism either results in increased glutamine consumption or decreased general metabolic activity. Further ACSS2i decreases glucose flux to α-KG, supporting the hypothesis that α-KG is an important source of citrate for acetylCoA production.

NAD^+ precursor NR did not result in an alteration of histone acetylation as measured by immunofluorescence staining, even though supplementation of NR was hypothesized to activate SIRT1, a known histone deacetylase that decreases its activity in AD neurons due to the lack of its cofactor NAD^+. Decreased SIRT1 activity has been concluded from increased histone acetylation and acetylation of CEBPα as measured previously by western blotting. To further characterize the functionality of SIRT1 and other deacetylases/acetyltransferases, we initiated mass-spectrometry based acetylomic analysis. One Million induced neurons of 9 patients and 9 controls were collected to prepare for proteomics analysis. Results from this experiment will uncover the state of histone acetylations and acetylations of other abundant proteins in the cells. Nevertheless, it will not be able to repeat this experiment with treated and non-treated cells, since the iNs approach does not result in high cell numbers and it is therefore not feasible to repeat the acetylomics approach with treatments. Nevertheless, we expect to find important metabolic regulators that show altered post translational modifications in form of acetylations that can be further analysed with the protein simple western blotting. NR treatement generally resulted in decreased metabolic activity, but could rescue the glucose flux to α-KG (Fig. 3). Reactive oxygen species have been suggested to play a big role in the reduction of glucose flux to α-KG by an inhibition of aconitase (69), which would be one way how NR, functioning as an antioxidant, could improve the α-KG/Citrate ratio. Besides NR, Shikonin could also improve α-KG production, suggesting an antioxidant role of that compound besides activating PKM2 (Fig. 6).

In summary our data reveals the interaction of metabolism and epigenetics in Alzheimer's disease. Our data suggests that by reverting parts of the metabolic switch, histone acetylation could be decreased, which may affect gene transcription. We identified compounds that successfully decrease glycolysis, increase glucose flux towards citrate into the TCA cycle, and decrease histone acetylation. The effects of the compounds on apoptosis competence and synapse formation is still to be evaluated in succeeding experiments.

Conclusion

Based on these pilot experiments, we conclude that a treatment with ACLYi, NR and shikonin or a combination of the three compounds should be further investigated using a bigger cohort, since especially ACLYi showed promising results to revert the metabolic switch, as well as effects on histone acetylation. Further, mass-spec based metabolomic analysis requires more cells to be able to detect metabolites like phosphoenolpyruvate, since with the duration of the treatment, cell loss results in low cell number at time of harvest.

Outlook

Samples have been prepared for evaluating CoA-metabolites, such as acetylCoA or malonylCoA, to further investigate the effects of AD on FAS. Further, the RedOx method will

be run on the samples to measure NAD species, such as NAD+, NADH, NADP+ or NADPH. However, due to technical problems with the instruments, the samples could not be analyzed so far. Additionally, acetylomics will be performed as soon as the instruments are up and running again. With the acetylomics we expect to see the hyperacetylation of specific histones as well as regulatory proteins of the metabolic switch, such as PKM or HIF1 α. Acetylation plays an essential role as post-translational modification and could be affected by a lack of sirtuin activity as well as over-abundance of acetylCoA.

Figures

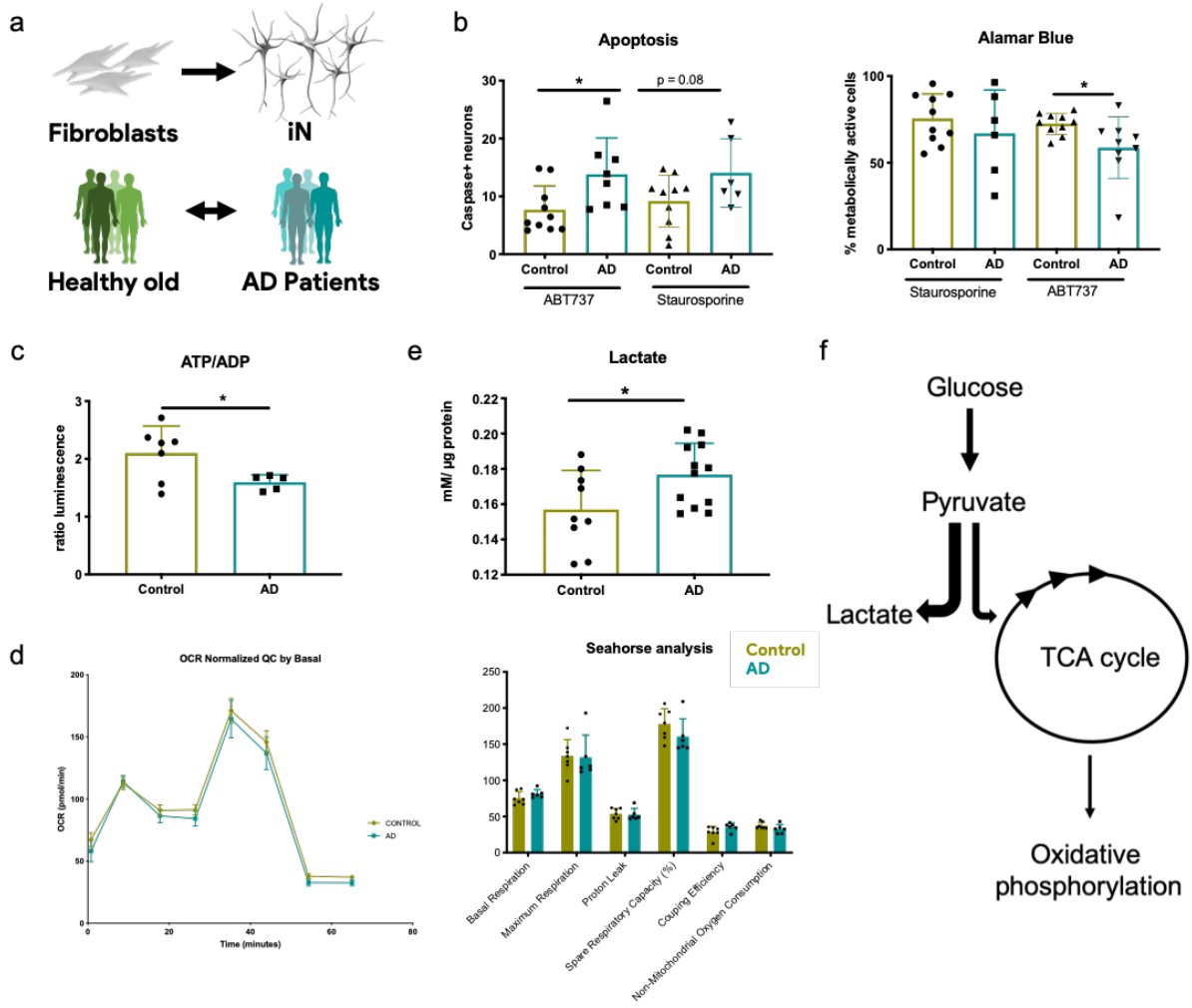

Figure 1. Energy status of de-differentiated AD iNs (a) Fibroblasts of AD patients and age-matched healthy control donors were directly converted to induced neurons. (b) Apoptosis competence was increased in AD iNs after 6-hour treatment with Bcl-2 inhibitor ABT-737 or protein kinase inhibitor staurosporine (*AD n=8, control n= 10, unpaired t-test).* Alamar Blue colorimetric measurement could further show a decrease of metabolically active cells after ABT-737 treatment. (c) An energy crisis could be observed in AD-iNs, as depicted in a decreased ATP/ADP ratio (*AD n=5, control n=7, unpaired t-test*), (d) which was not caused by dysfunctional mitochondria (*AD n=6, control n=7, unpaired t-test*). (e,f) Similar to the Warburg effect, Lactate production was increased in AD iNs (*AD n=12, control n=9, unpaired t-test*).

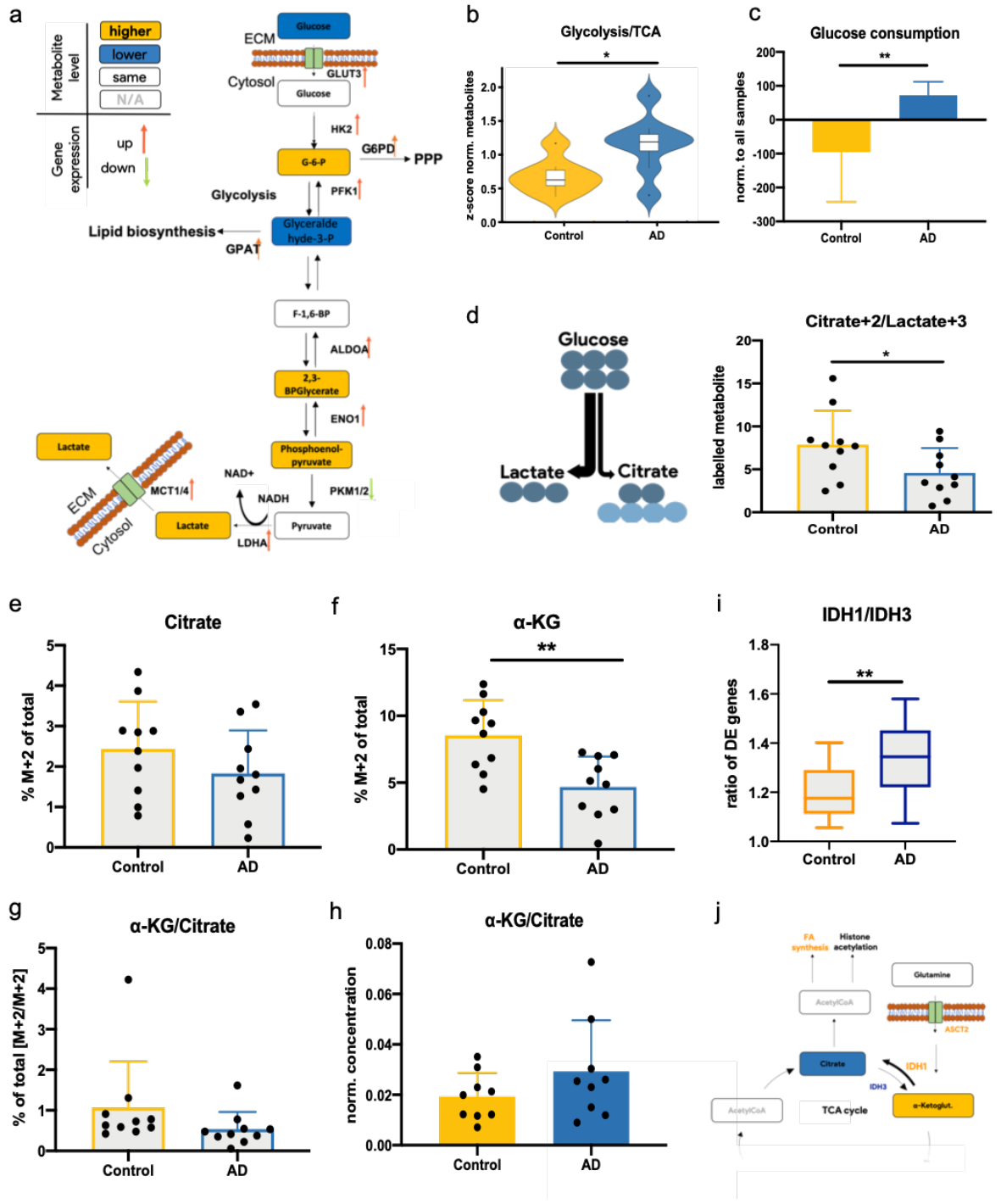

Figure 2. Metabolic switch in AD iNs (a) MS-based metabolomics of 10 control and 10 AD iNs showed an accumulation of glycolytic metabolites in the cells and decreased glucose and increased lactate in the supernatants. Gene expression of enzymes involved in glycolytic pathways were significantly increased. (b) AD iN showed increased metabolites of glycolytic pathway compared to TCA cycle as shown in the ratio of z-scores of all metabolites except for glucose involved. (c) AD iNs took up more glucose compared to control iNs as shown by the reduction of glucose in the supernatant. (d) Schematic drawing and graph showing glucose utilization was directed towards lactate in AD and away from citrate production and the TCA cycle as quantified by the incorporation of C_{13} derived from $^{6}C_{13}$-labelled glucose. (e) Glucose

flux to citrate was slightly decreased in AD iNs, (f, g) resulting citrate was less efficiently metabolized further to α-KG. (h) This block of glucose metabolism was not observed on total metabolite level, which showed more total α-KG per citrate. (i) Transcriptomic analysis further supports this observation with an increased IDH1/IDH3 ratio, (j) where increased IDH1 expression increases citrate production from α-KG to support protein acetylation and FAS. (*AD n=10, control n=10, unpaired t-test *p<0.05, **p<0.001)*

Figure 3. NR treatment partially reverts the metabolic switch (a) RNA expression of NAD biosynthesis related genes were significantly increased in sporadic AD iNs, (b) whereas total free NAD^+ levels were decreased (*AD n=12, control n=12, unpaired t-test *p<0.05)*. (c) Control and AD iNs were treated with NR, a NAD^+ precursor, for 3 days. (d) Despite showing positive effects on control cells, NR triggered extensive cell death in AD iNs of patient #2800. (e) NR slightly increased glycolysis/TCA ratio in both control and AD iNs, (f) but could decrease lactate excretion and glucose consumption in AD iNs. (g) MS-based metabolome analysis showed a decrease of most glycolytic intermediates, however 2/3-biphospho-glycerate was accumulated. (h) α-KG levels could be almost doubled, whereas other TCA cycle intermediates were mainly unaffected by NR treatment. (i) These effects on glycolysis and TCA cycle could also be shown in a decreased ratio of lactate per citrate or lactate per glucose and additionally α-KG per citrate was elevated. (j) glucose flux into the TCA cycle was slightly elevated as shown by the ratio of labelled citrate to lactate (M+2 per M+3). Further citrate is further metabolized to α-KG.

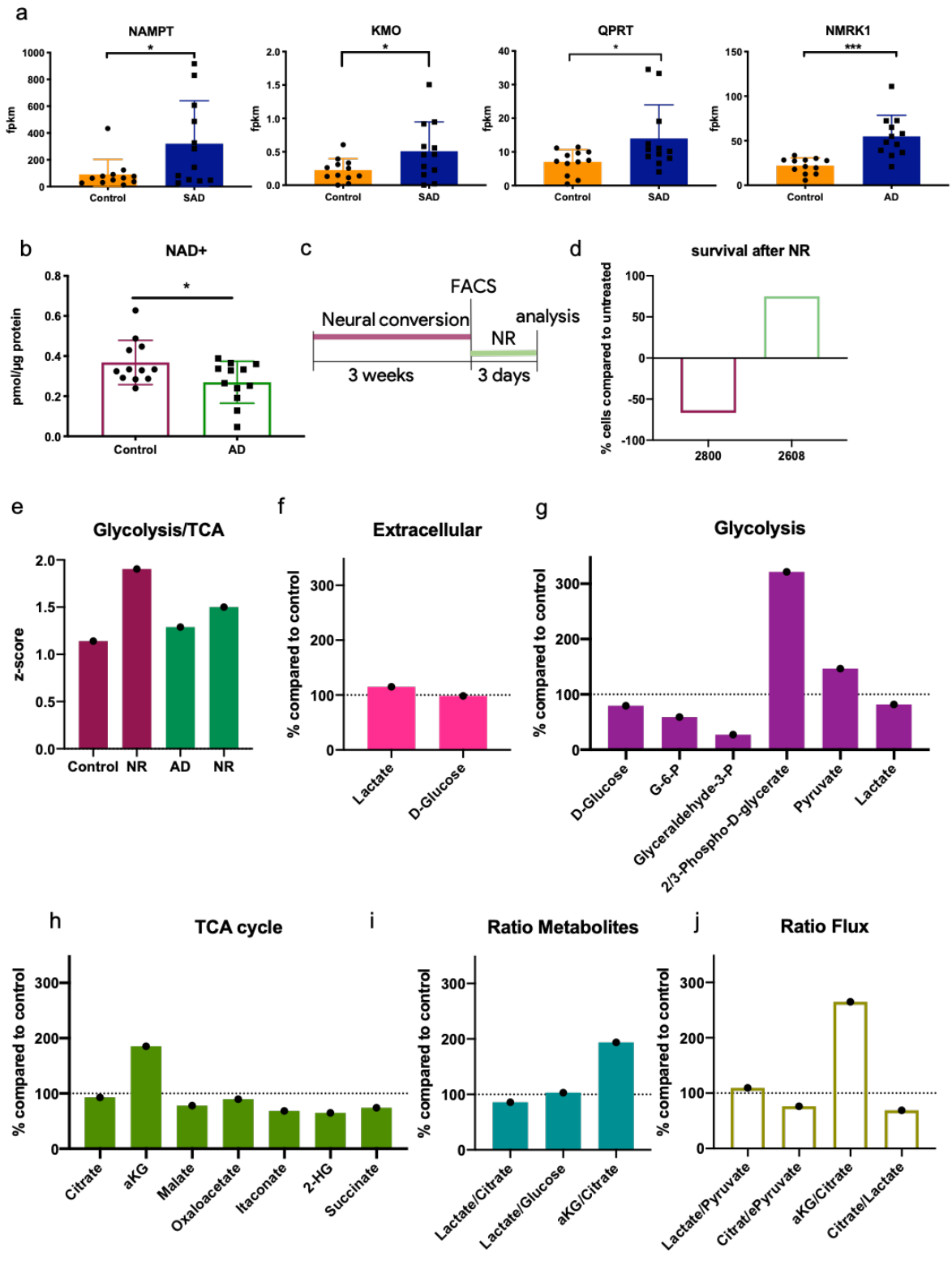
a
NAMPT
KMO
QPRT
NMRK1
fpkm
Control
SAD
AD
b
NAD+
pmol/µg protein
c
FACS
Neural conversion
analysis
NR
3 weeks
3 days
d
survival after NR
% cells compared to untreated
2800
2608
e
Glycolysis/TCA
z-score
Control
NR
AD
f
Extracellular
% compared to control
Lactate
D-Glucose
g
Glycolysis
D-Glucose
G-6-P
Glyceraldehyde-3-P
2/3-Phospho-D-glycerate
Pyruvate
Lactate
h
TCA cycle
Citrate
aKG
Malate
Oxaloacetate
Itaconate
2-HG
Succinate
i
Ratio Metabolites
Lactate/Citrate
Lactate/Glucose
aKG/Citrate
j
Ratio Flux
Lactate/Pyruvate
Citrat/ePyruvate
aKG/Citrate
Citrate/Lactate

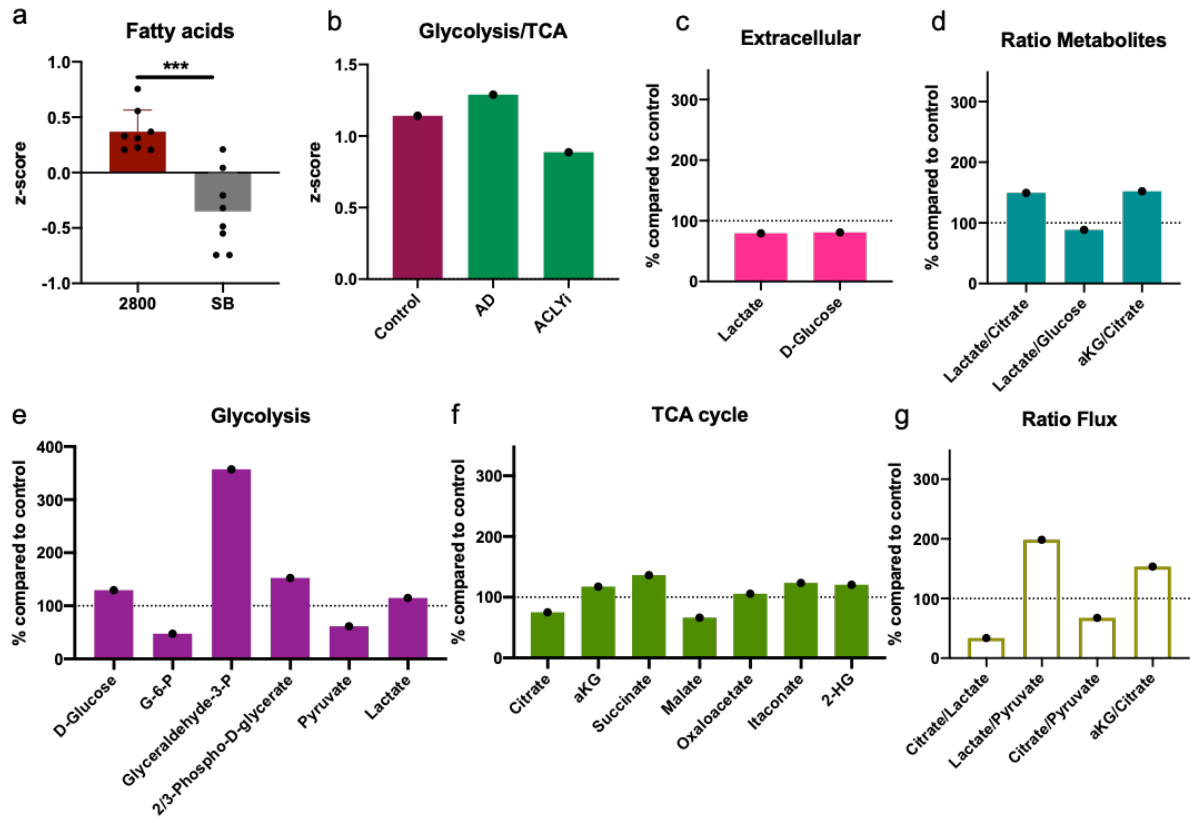

Figure 4. Effects of ACLY inhibition on the metabolic switch (a) ACLY inhibition could decrease all eight fatty acids measured by the mass spectrometry method applied, supporting the functionality of the inhibitor. (b) ACLYi was only tested on AD cells, where it could decrease the glycolysis/TCA ratio, (c) lactate excretion and glucose consumption. (d) Treated cells were still mainly glycolytic as shown in the increased lactate/citrate ratios. (e) Glycolytic metabolites could be partially decreased, (f) whereas TCA cycle intermediates were increased. (g) Glucose was mainly metabolized to lactate, however the citrate produced from glucose could be further metabolized to α-KG.

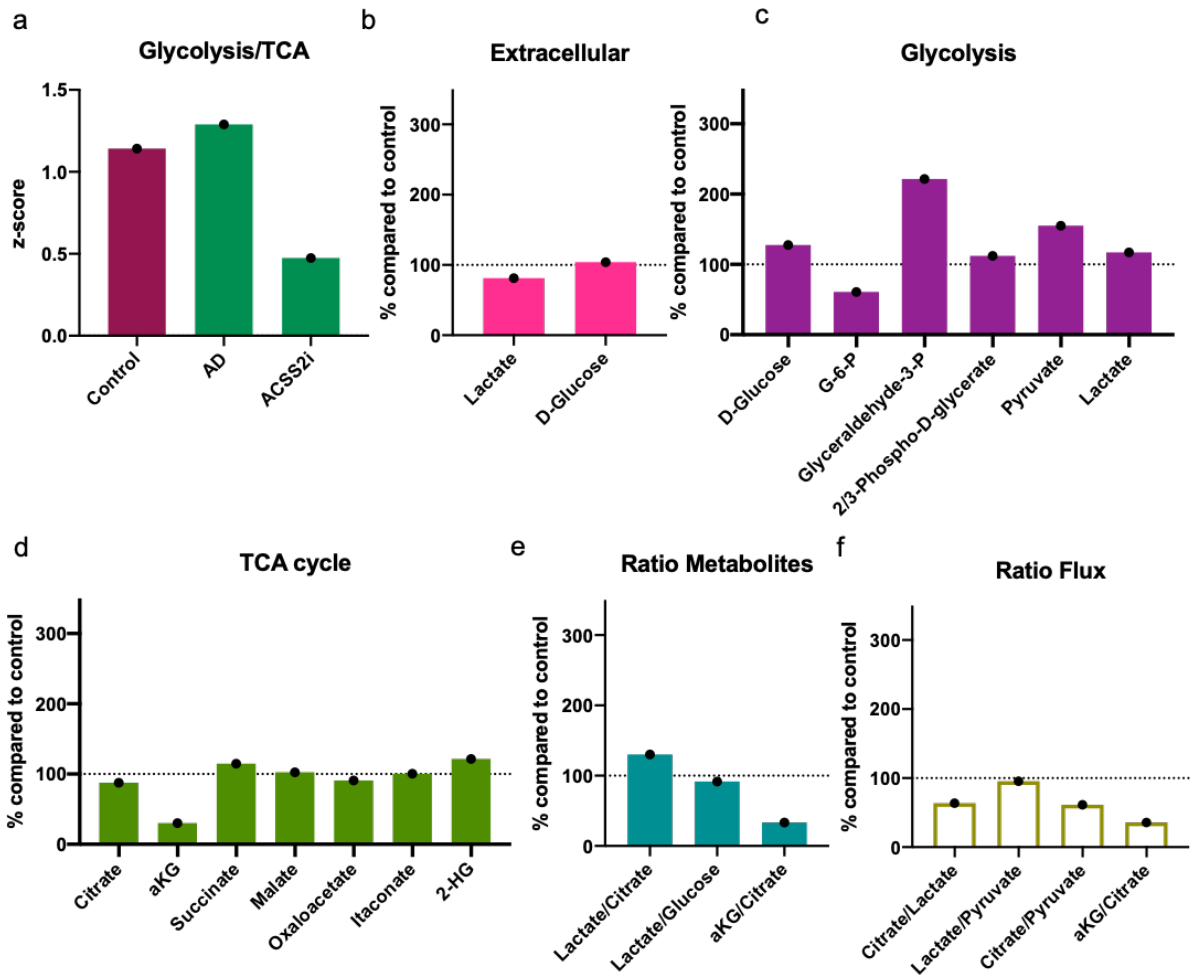

Figure 5. Effects of ACSS2i on AD iNs (a) ACLY inhibition decreased the glycolysis/TCA ratio, (b) lactate excretion and glucose consumption. (c) Glycolytic metabolites reached levels close to control cells, (d) as well as all TCA cycle intermediates except for α-KG displayed normal control levels. (d) Blockade of α-KG production from citrate is shown in total metabolite and glucose-derived C_{13}-labelled metabolites.

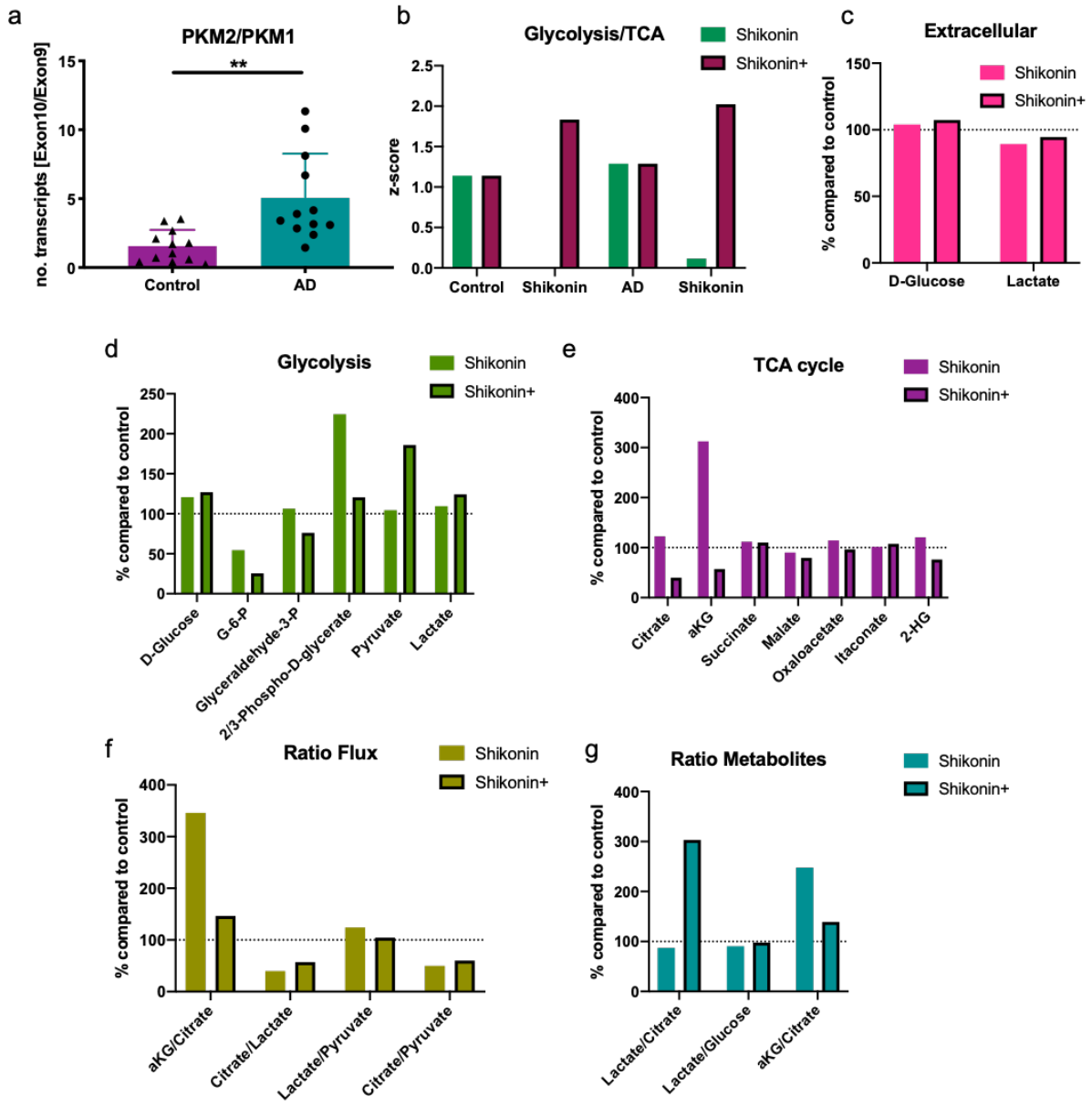

Figure 6. Shikonin with and without NR successfully revert many aspects of the metabolic switch (a) RNA-seq revealed an increase of the inactive PKM2 isoform. (b) Treatment with Shikonin can activate PKM2, decreasing glycolysis/TCA ratio in AD iNs. The addition of NR reverted this decrease, (c) whereas both conditions could normalize glucose consumption and lactate production, (d,e) decreased glycolytic metabolites and Shikonin alone additionally brought citrate and α-KG levels to a normal or even increased level. (f) Glucose flux to α-KG was increased, (g) resulting in a restored ratio of α-KG/citrate.

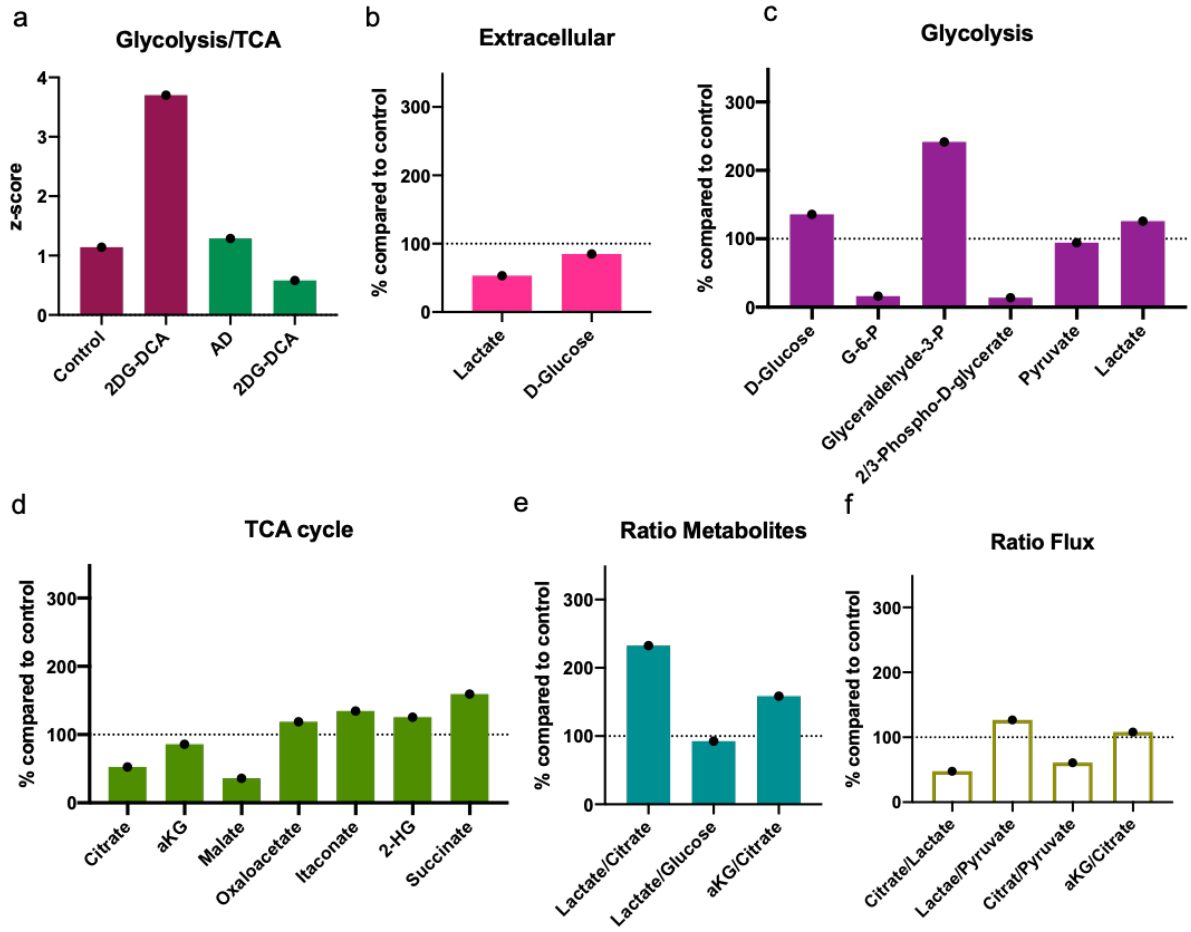

Figure 7. 2-Deoxyglucose and dichloroacetate treatment decreased metabolic activity of AD iNs (a) 2DG/DCA treatment resulted in an increase in glycolysis/TCA ratio in control iNs, but in a decrease in AD iNs. (b) Lactate excretion and glucose consumption could be decreased upon treatment, (c) but intracellular lactate was still increased. Some of the glycolytic and (d) TCA cycle metabolites were highly decreased, (e) but cells were still rather glycolytic. (f) Glucose flux to citrate was still low, and most C_{13} was directed towards lactate, suggesting that DCA did not exert its function.

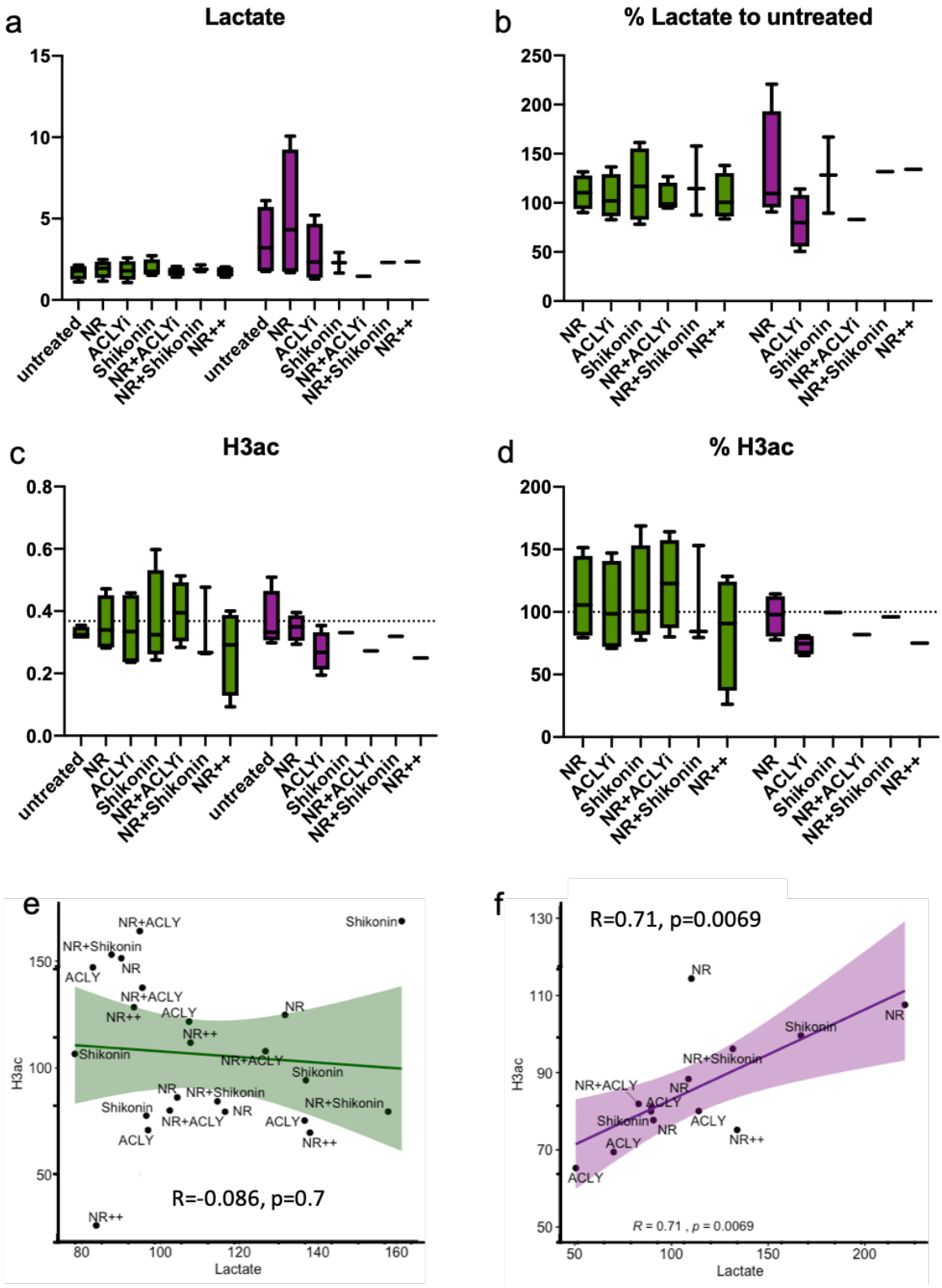

Figure 8. Interaction of Metabolism and Epigenetics (a) Total Lactate levels and (b) percentage compared to untreated control or AD iNs, respectively, were measured upon treatment with NR, ACLYi, Shikonin or a combination. Only ACLYi and combinations with ACLYi were able to reduce Lactate levels compared to untreated iNs. (c) Histone acetylation of the same cells was measured by immunostaining, were ACLYi was the only compound

successfully decreasing H3ac levels. (e,f) A correlation of metabolic changes and histone acetylation upon treatment was only found in AD iNs, but not in control iNs, suggesting that the compounds applied do not affect healthy cells.

Supplementary Figure 1. (a) Metabolic Profile of AD iNs versus control iNs. (b) Heavy labelled glucose is taken up equally throughout all treatment conditions. (c) Citrate M+2, M+3 or M+4 change with different treatments, suggesting increased citrate derived from glucose, citrate produced through glucose-dependent aneplerosis or increased TCA cycle activity, respectively. (c) NR restored glucose contribution to 6-phosphogluconate. (e) Previous experiment could show that AD iNs are more glycolytic, using glucose for glycolysis rather than citrate production. (f) RNA-Seq analysis revelaed an increased ratio of IDH1/IDH3, suggesting increased citrate production from α-KG. (g) Glucose tracing showed that less α-KG is derived from glucose in AD iNs. (h) Transcriptomic analysis showed an upregulation of genes involved in FAS, (i) and immunostaining showed increased histone 3 acetylation in AD iNs. (j) 2DG/DCA treated control iNs decrease most of their glycolytic metabolites, pyruvate, however, is highly increased, resulting in increased glycolysis/TCA ratio.

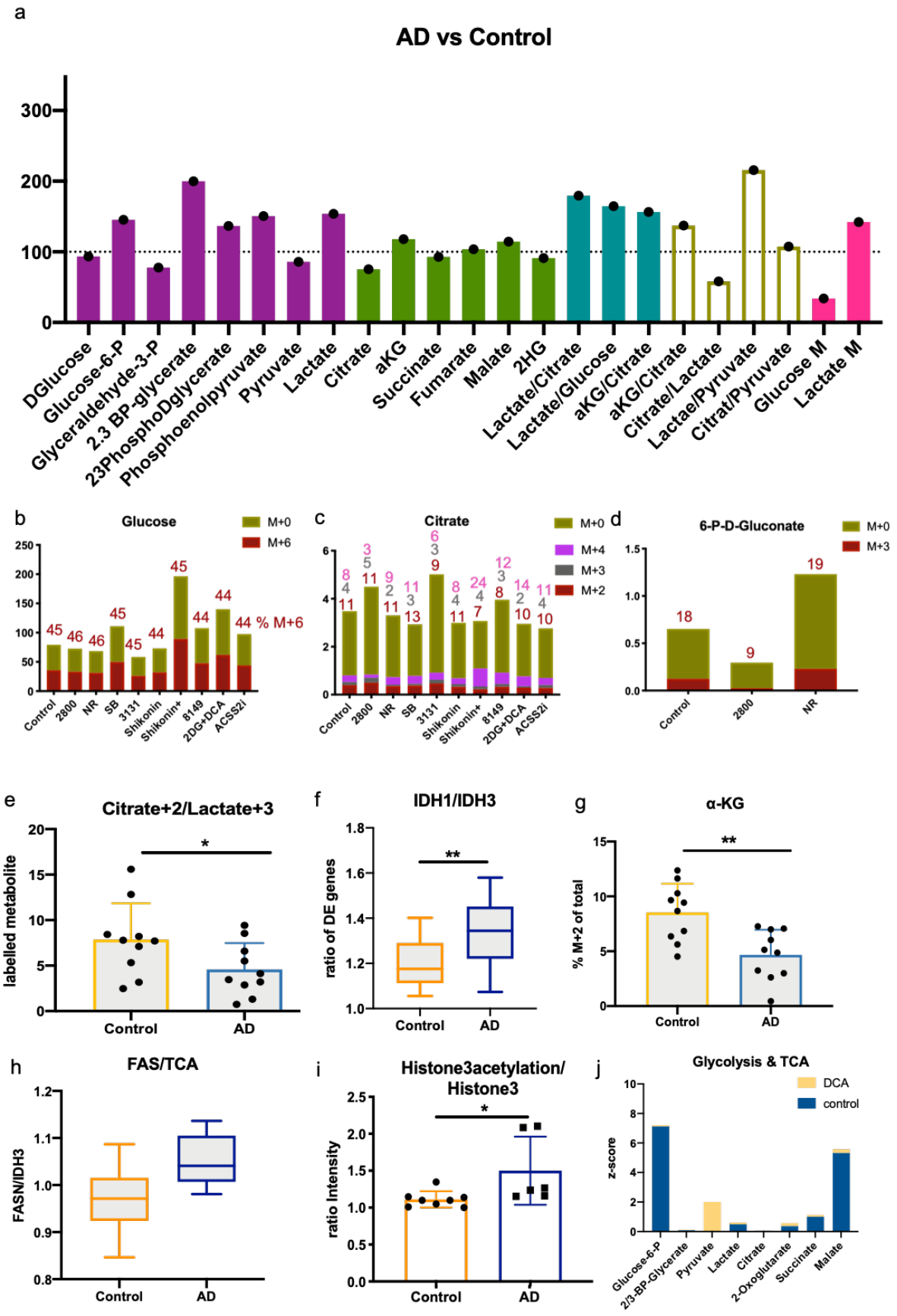
a
AD vs Control
DGlucose
Glucose-6-P
Glyceraldehyde-3-P
2.3 BP-glycerate
23PhosphoDglycerate
Phosphoenolpyruvate
Pyruvate
Lactate
Citrate
aKG
Succinate
Fumarate
Malate
2HG
Lactate/Citrate
Lactate/Glucose
aKG/Citrate
aKG/Citrate
Citrate/Lactate
Lactae/Pyruvate
Citrat/Pyruvate
Glucose M
Lactate M
b
Glucose
M+0
M+6
% M+6
Control
2800
NR
SB
3131
Shikonin
Shikonin+
8149
2DG+DCA
ACSS2i
c
Citrate
M+0
M+4
M+3
M+2
d
6-P-D-Gluconate
M+0
M+3
e
Citrate+2/Lactate+3
labelled metabolite
Control
AD
f
IDH1/IDH3
ratio of DE genes
g
α-KG
% M+2 of total
h
FAS/TCA
FASN/IDH3
i
Histone3acetylation/
Histone3
ratio Intensity
j
Glycolysis & TCA
DCA
control
z-score
Glucose-6-P
2/3-BP-Glycerate
Pyruvate
Lactate
Citrate
2-Oxoglutarate
Succinate
Malate

References

1. International D. World Alzheimer Report 2018 - The state of the art of dementia research: New frontiers; World Alzheimer Report 2018 - The state of the art of dementia research: New frontiers [Internet]. [cited 2020 Jan 6]. Available from: https://www.alz.co.uk/research/WorldAlzheimerReport2018.pdf
2. Hall AM, Roberson ED. Mouse models of Alzheimer's disease. Brain Res Bull [Internet]. 2012 May 1 [cited 2020 Jan 6];88(1):3–12. Available from: http://www.ncbi.nlm.nih.gov/pubmed/22142973
3. Alzheimer's Association. 2016 Alzheimer's disease facts and figures. Alzheimer's Dement [Internet]. 2016 Apr [cited 2019 Nov 13];12(4):459–509. Available from: http://www.ncbi.nlm.nih.gov/pubmed/27570871
4. Herrup K. The case for rejecting the amyloid cascade hypothesis. Nat Neurosci [Internet]. 2015 Jun 26 [cited 2020 Feb 26];18(6):794–9. Available from: http://www.nature.com/articles/nn.4017
5. Liu X, Jiao B, Shen L. The Epigenetics of Alzheimer's Disease: Factors and Therapeutic Implications. Front Genet [Internet]. 2018 Nov 30 [cited 2020 Feb 26];9:579. Available from: https://www.frontiersin.org/article/10.3389/fgene.2018.00579/full
6. Inda MC, Joshi S, Wang T, Bolaender A, Gandu S, Koren III J, et al. The epichaperome is a mediator of toxic hippocampal stress and leads to protein connectivity-based dysfunction. Nat Commun [Internet]. 2020 Dec 16 [cited 2020 Feb 26];11(1):319. Available from: http://www.nature.com/articles/s41467-019-14082-5
7. Frobel J, Hemeda H, Lenz M, Abagnale G, Joussen S, Denecke B, et al. Epigenetic Rejuvenation of Mesenchymal Stromal Cells Derived from Induced Pluripotent Stem Cells. Stem Cell Reports [Internet]. 2014 Sep 9 [cited 2018 Oct 1];3(3):414–22. Available from: http://www.ncbi.nlm.nih.gov/pubmed/25241740
8. Lapasset L, Milhavet O, Prieur A, Besnard E, Babled A, Aït-Hamou N, et al. Rejuvenating senescent and centenarian human cells by reprogramming through the pluripotent state. Genes Dev [Internet]. 2011 Nov 1 [cited 2019 Aug 12];25(21):2248–53. Available from: http://www.ncbi.nlm.nih.gov/pubmed/22056670
9. Mertens J, Paquola ACM, Ku M, Hatch E, Böhnke L, Ladjevardi S, et al. Directly Reprogrammed Human Neurons Retain Aging-Associated Transcriptomic Signatures and Reveal Age-Related Nucleocytoplasmic Defects. Cell Stem Cell [Internet]. 2015 Dec 3 [cited 2018 Apr 24];17(6):705–18. Available from: http://www.ncbi.nlm.nih.gov/pubmed/26456686
10. Takahashi K, Tanabe K, Ohnuki M, Narita M, Ichisaka T, Tomoda K, et al. Induction of pluripotent stem cells from adult human fibroblasts by defined factors. Cell [Internet]. 2007 Nov 30 [cited 2018 Aug 29];131(5):861–72. Available from: http://www.ncbi.nlm.nih.gov/pubmed/18035408
11. Huh CJ, Zhang B, Victor MB, Dahiya S, Batista LF, Horvath S, et al. Maintenance of age in human neurons generated by microRNA-based neuronal conversion of fibroblasts. Elife [Internet]. 2016 Sep 20 [cited 2018 Aug 30];5. Available from: https://elifesciences.org/articles/18648
12. Zheng X, Boyer L, Jin M, Mertens J, Kim Y, Ma L, et al. Metabolic reprogramming during neuronal differentiation from aerobic glycolysis to neuronal oxidative phosphorylation. Elife [Internet]. 2016 Jun 10 [cited 2018 Sep 1];5. Available from: https://elifesciences.org/articles/13374
13. Traxler L, Edenhofer F, Mertens J. Next-generation disease modeling with direct

conversion: A new path to old neurons. FEBS Lett [Internet]. 2019 Nov 12 [cited 2019 Nov 13];1873-3468.13678. Available from: https://onlinelibrary.wiley.com/doi/abs/10.1002/1873-3468.13678
14. Sonntag K-C, Ryu W-I, Amirault KM, Healy RA, Siegel AJ, McPhie DL, et al. Late-onset Alzheimer's disease is associated with inherent changes in bioenergetics profiles. Sci Rep [Internet]. 2017 Dec 25 [cited 2019 Nov 13];7(1):14038. Available from: http://www.nature.com/articles/s41598-017-14420-x
15. Feng Z, Hanson RW, Berger NA, Trubitsyn A. Reprogramming of energy metabolism as a driver of aging [Internet]. Vol. 7. 2016 [cited 2019 Nov 13]. Available from: www.impactjournals.com/oncotarget
16. Raichle ME, Gusnard DA. Appraising the brain's energy budget. Proc Natl Acad Sci U S A [Internet]. 2002 Aug 6 [cited 2019 Nov 14];99(16):10237–9. Available from: http://www.ncbi.nlm.nih.gov/pubmed/12149485
17. Vander Heiden MG, Cantley LC, Thompson CB. Understanding the Warburg Effect: The Metabolic Requirements of Cell Proliferation. Science (80-) [Internet]. 2009 May 22 [cited 2018 Sep 1];324(5930):1029–33. Available from: http://www.sciencemag.org/cgi/doi/10.1126/science.1160809
18. Pavlova NN, Thompson CB. The Emerging Hallmarks of Cancer Metabolism. Cell Metab [Internet]. 2016 Jan 12 [cited 2019 Nov 13];23(1):27–47. Available from: https://linkinghub.elsevier.com/retrieve/pii/S155041311500621X
19. Galluzzi L, Kepp O, Heiden MG Vander, Kroemer G. Metabolic targets for cancer therapy. Nat Rev Drug Discov [Internet]. 2013 Nov 11 [cited 2019 Nov 14];12(11):829–46. Available from: http://www.nature.com/articles/nrd4145
20. Caldwell AB, Liu Q, Schroth GP, Tanzi RE, Galasko DR, Yuan SH, et al. Dedifferentiation orchestrated through remodeling of the chromatin landscape defines PSEN1 mutation-induced Alzheimer's Disease. bioRxiv [Internet]. 2019 Jan 29 [cited 2019 Nov 14];531202. Available from: https://www.biorxiv.org/content/10.1101/531202v1
21. Sánchez-Valle J, Tejero H, Ibáñez K, Portero JL, Krallinger M, Al-Shahrour F, et al. A molecular hypothesis to explain direct and inverse co-morbidities between Alzheimer's Disease, Glioblastoma and Lung cancer. Sci Rep [Internet]. 2017 Dec 30 [cited 2019 Nov 14];7(1):4474. Available from: http://www.nature.com/articles/s41598-017-04400-6
22. Benn SC, Woolf CJ. Adult neuron survival strategies — slamming on the brakes. Nat Rev Neurosci [Internet]. 2004 Sep [cited 2019 Nov 15];5(9):686–700. Available from: http://www.ncbi.nlm.nih.gov/pubmed/15322527
23. Folch J, Junyent F, Verdaguer E, Auladell C, Pizarro JG, Beas-Zarate C, et al. Role of Cell Cycle Re-Entry in Neurons: A Common Apoptotic Mechanism of Neuronal Cell Death. Neurotox Res [Internet]. 2012 Oct 1 [cited 2019 Nov 15];22(3):195–207. Available from: http://www.ncbi.nlm.nih.gov/pubmed/21965004
24. Barrio-Alonso E, Hernández-Vivanco A, Walton CC, Perea G, Frade JM. Cell cycle reentry triggers hyperploidization and synaptic dysfunction followed by delayed cell death in differentiated cortical neurons. Sci Rep [Internet]. 2018 Dec 25 [cited 2019 Nov 15];8(1):14316. Available from: http://www.nature.com/articles/s41598-018-32708-4
25. Mosconi L. Glucose metabolism in normal aging and Alzheimer's disease: Methodological and physiological considerations for PET studies. Clin Transl imaging [Internet]. 2013 Aug [cited 2019 Nov 15];1(4). Available from:

http://www.ncbi.nlm.nih.gov/pubmed/24409422
26. Xu J, Begley P, Church SJ, Patassini S, McHarg S, Kureishy N, et al. Elevation of brain glucose and polyol-pathway intermediates with accompanying brain-copper deficiency in patients with Alzheimer's disease: metabolic basis for dementia. Sci Rep [Internet]. 2016 [cited 2019 Nov 15];6:27524. Available from: http://www.ncbi.nlm.nih.gov/pubmed/27276998
27. Yucel N, Wang YX, Mai T, Porpiglia E, Lund PJ, Markov G, et al. Glucose Metabolism Drives Histone Acetylation Landscape Transitions that Dictate Muscle Stem Cell Function. Cell Rep [Internet]. 2019 [cited 2020 Mar 13];27(13):3939-3955.e6. Available from: http://www.ncbi.nlm.nih.gov/pubmed/31242425
28. Alistar A, Morris BB, Desnoyer R, Klepin HD, Hosseinzadeh K, Clark C, et al. Safety and tolerability of the first-in-class agent CPI-613 in combination with modified FOLFIRINOX in patients with metastatic pancreatic cancer: a single-centre, open-label, dose-escalation, phase 1 trial. Lancet Oncol [Internet]. 2017 [cited 2019 Nov 15];18(6):770–8. Available from: http://www.ncbi.nlm.nih.gov/pubmed/28495639
29. da Veiga Moreira J, Hamraz M, Abolhassani M, Schwartz L, Jolicœur M, Peres S. Metabolic therapies inhibit tumor growth in vivo and in silico. Sci Rep [Internet]. 2019 Dec 28 [cited 2019 Nov 15];9(1):3153. Available from: http://www.nature.com/articles/s41598-019-39109-1
30. Hou Y, Lautrup S, Cordonnier S, Wang Y, Croteau DL, Zavala E, et al. NAD $^{+}$ supplementation normalizes key Alzheimer's features and DNA damage responses in a new AD mouse model with introduced DNA repair deficiency. Proc Natl Acad Sci [Internet]. 2018 Feb 20 [cited 2019 Nov 13];115(8):E1876–85. Available from: http://www.ncbi.nlm.nih.gov/pubmed/29432159
31. Lautrup S, Sinclair DA, Mattson MP, Fang EF. NAD+ in Brain Aging and Neurodegenerative Disorders. Cell Metab [Internet]. 2019 Oct 1 [cited 2020 Feb 26];30(4):630–55. Available from: https://www.sciencedirect.com/science/article/pii/S1550413119305029?via%3Dihub
32. Bertoldo MJ, Listijono DR, Ho W-HJ, Riepsamen AH, Goss DM, Richani D, et al. NAD+ Repletion Rescues Female Fertility during Reproductive Aging. Cell Rep [Internet]. 2020 Feb 11 [cited 2020 Feb 26];30(6):1670-1681.e7. Available from: https://www.sciencedirect.com/science/article/pii/S2211124720300838?via%3Dihub
33. Rajman L, Chwalek K, Sinclair DA. Therapeutic Potential of NAD-Boosting Molecules: The In Vivo Evidence. Cell Metab [Internet]. 2018 [cited 2020 Feb 26];27(3):529–47. Available from: http://www.ncbi.nlm.nih.gov/pubmed/29514064
34. Zhang H, Wang D, Li M, Plecitá-Hlavatá L, D'Alessandro A, Tauber J, et al. Metabolic and Proliferative State of Vascular Adventitial Fibroblasts in Pulmonary Hypertension Is Regulated Through a MicroRNA-124/PTBP1 (Polypyrimidine Tract Binding Protein 1)/Pyruvate Kinase Muscle Axis. Circulation [Internet]. 2017 Dec 19 [cited 2019 Nov 18];136(25):2468–85. Available from: http://www.ncbi.nlm.nih.gov/pubmed/28972001
35. Uguccioni M, Allavena P, Alves-Filho JC, Br; J, Pålsson-Mcdermott EM. Pyruvate Kinase M2: A Potential Target for Regulating inflammation. 2016 [cited 2020 Feb 27];7:1. Available from: www.frontiersin.org
36. Sivanand S, Viney I, Wellen KE. Spatiotemporal Control of Acetyl-CoA Metabolism in Chromatin Regulation. Trends Biochem Sci [Internet]. 2018 [cited 2020 Feb 27];43(1):61–74. Available from: https://doi.org/10.1016/j.tibs.2017.11.004

37. Gao X, Lin S-H, Ren F, Li J-T, Chen J-J, Yao C-B, et al. Acetate functions as an epigenetic metabolite to promote lipid synthesis under hypoxia. Nat Commun [Internet]. 2016 Jun 30 [cited 2018 Oct 25];7:11960. Available from: http://www.nature.com/doifinder/10.1038/ncomms11960
38. Granchi C. ATP citrate lyase (ACLY) inhibitors: An anti-cancer strategy at the crossroads of glucose and lipid metabolism. Eur J Med Chem [Internet]. 2018 Sep 5 [cited 2020 Jan 9];157:1276–91. Available from: http://www.ncbi.nlm.nih.gov/pubmed/30195238
39. Wen H, Lee S, Zhu W-G, Lee O-J, Yun SJ, Kim J, et al. Glucose-derived acetate and ACSS2 as key players in cisplatin resistance in bladder cancer. Biochim Biophys Acta - Mol Cell Biol Lipids [Internet]. 2019 Mar [cited 2020 Feb 27];1864(3):413–21. Available from: http://www.ncbi.nlm.nih.gov/pubmed/29883801
40. Khwairakpam A, Shyamananda M, Sailo B, Rathnakaram S, Padmavathi G, Kotoky J, et al. ATP Citrate Lyase (ACLY): A Promising Target for Cancer Prevention and Treatment. Curr Drug Targets [Internet]. 2015 Feb 9 [cited 2019 Nov 18];16(2):156–63. Available from: http://www.ncbi.nlm.nih.gov/pubmed/25537655
41. Schug ZT, Peck B, Jones DT, Zhang Q, Grosskurth S, Alam IS, et al. Article Acetyl-CoA Synthetase 2 Promotes Acetate Utilization and Maintains Cancer Cell Growth under Metabolic Stress. Cancer Cell [Internet]. 2015 [cited 2019 Nov 18];27:57–71. Available from: http://dx.doi.org/10.1016/j.ccell.2014.12.002
42. Michelakis ED, Webster L, Mackey JR. Dichloroacetate (DCA) as a potential metabolic-targeting therapy for cancer. Br J Cancer [Internet]. 2008 Oct 7 [cited 2019 Nov 18];99(7):989–94. Available from: http://www.ncbi.nlm.nih.gov/pubmed/18766181
43. He L, Diedrich J, Chu Y-Y, Yates JR. Extracting Accurate Precursor Information for Tandem Mass Spectra by RawConverter. Anal Chem [Internet]. 2015 Nov 17 [cited 2019 Oct 22];87(22):11361–7. Available from: http://www.ncbi.nlm.nih.gov/pubmed/26499134
44. Luo C, Lee QY, Wapinski O, Castanon R, Nery JR, Mall M, et al. Global DNA methylation remodeling during direct reprogramming of fibroblasts to neurons. Elife [Internet]. 2019 Jan 15 [cited 2019 Jan 24];8. Available from: https://elifesciences.org/articles/40197
45. Kim Y, Zheng X, Ansari Z, Bunnell MC, Herdy JR, Traxler L, et al. Mitochondrial Aging Defects Emerge in Directly Reprogrammed Human Neurons due to Their Metabolic Profile. Cell Rep [Internet]. 2018 May 29 [cited 2019 Feb 4];23(9):2550–8. Available from: https://www.sciencedirect.com/science/article/pii/S2211124718307034
46. Maldonado EN, Lemasters JJ. ATP/ADP ratio, the missed connection between mitochondria and the Warburg effect. Mitochondrion [Internet]. 2014 Nov [cited 2020 Feb 27];19 Pt A:78–84. Available from: http://www.ncbi.nlm.nih.gov/pubmed/25229666
47. Caruso P, Dunmore BJ, Schlosser K, Schoors S, Dos Santos C, Perez-Iratxeta C, et al. Identification of MicroRNA-124 as a Major Regulator of Enhanced Endothelial Cell Glycolysis in Pulmonary Arterial Hypertension via PTBP1 (Polypyrimidine Tract Binding Protein) and Pyruvate Kinase M2. Circulation [Internet]. 2017 Dec 19 [cited 2020 Mar 17];136(25):2451–67. Available from: http://www.ncbi.nlm.nih.gov/pubmed/28971999
48. Mouchiroud L, Houtkooper RH, Moullan N, Katsyuba E, Ryu D, Cantó C, et al. The NAD+/Sirtuin Pathway Modulates Longevity through Activation of Mitochondrial UPR

and FOXO Signaling. Cell [Internet]. 2013 Jul 18 [cited 2019 Nov 14];154(2):430–41. Available from: https://www.sciencedirect.com/science/article/pii/S0092867413007551?via%3Dihub
49. Schultz MB, Sinclair DA. Why NAD + Declines during Aging: It's Destroyed HHS Public Access. Cell Metab [Internet]. 2016 [cited 2019 Nov 15];23(6):965–6. Available from: http://dx.doi.org/10.1126/
50. Houtkooper RH, Pirinen E, Auwerx J. Sirtuins as regulators of metabolism and healthspan. Nat Rev Mol Cell Biol [Internet]. 2012 Mar 7 [cited 2019 Nov 14];13(4):225–38. Available from: http://www.ncbi.nlm.nih.gov/pubmed/22395773
51. Chen P-H, Cai L, Huffman K, Yang C, Kim J, Faubert B, et al. Metabolic Diversity in Human Non-Small Cell Lung Cancer Cells. Mol Cell [Internet]. 2019 Dec 5 [cited 2020 Mar 3];76(5):838-851.e5. Available from: https://www.sciencedirect.com/science/article/pii/S1097276519306835?via%3Dihub
52. Banerjee DR, Deckard CE, Zeng Y, Sczepanski JT. Acetylation of the histone H3 tail domain regulates base excision repair on higher-order chromatin structures. Sci Rep [Internet]. 2019 Dec 4 [cited 2020 Mar 4];9(1):15972. Available from: http://www.nature.com/articles/s41598-019-52340-0
53. Hynes MJ, Murray SL. ATP-citrate lyase is required for production of cytosolic acetyl coenzyme A and development in Aspergillus nidulans. Eukaryot Cell [Internet]. 2010 Jul 1 [cited 2020 Jan 9];9(7):1039–48. Available from: http://www.ncbi.nlm.nih.gov/pubmed/20495057
54. Granchi C. ATP citrate lyase (ACLY) inhibitors: An anti-cancer strategy at the crossroads of glucose and lipid metabolism. Eur J Med Chem [Internet]. 2018 Sep 5 [cited 2018 Oct 25];157:1276–91. Available from: http://www.ncbi.nlm.nih.gov/pubmed/30195238
55. Shah S, Carriveau WJ, Li J, Campbell SL, Kopinski PK, Lim H-W, et al. Targeting ACLY sensitizes castration-resistant prostate cancer cells to AR antagonism by impinging on an ACLY-AMPK-AR feedback mechanism. Oncotarget [Internet]. 2016 Jul 12 [cited 2020 Jan 9];7(28):43713–30. Available from: http://www.ncbi.nlm.nih.gov/pubmed/27248322
56. Zlotorynski E. ACSS2 boosts local histone acetylation. Nat Rev Mol Cell Biol [Internet]. 2017 Jul 7 [cited 2020 Mar 4];18(7):405–405. Available from: http://www.nature.com/articles/nrm.2017.61
57. Schug ZT, Peck B, Jones DT, Zhang Q, Grosskurth S, Alam IS, et al. Acetyl-CoA Synthetase 2 Promotes Acetate Utilization and Maintains Cancer Cell Growth under Metabolic Stress. Cancer Cell [Internet]. 2015 Jan 12 [cited 2020 Mar 4];27(1):57–71. Available from: http://www.ncbi.nlm.nih.gov/pubmed/25584894
58. Cortés-Cros M, Hemmerlin C, Ferretti S, Zhang J, Gounarides JS, Yin H, et al. M2 isoform of pyruvate kinase is dispensable for tumor maintenance and growth. [cited 2019 Nov 19]; Available from: www.pnas.org/cgi/doi/10.1073/pnas.1212780110
59. Alves-Filho JC, Pålsson-McDermott EM. Pyruvate Kinase M2: A Potential Target for Regulating Inflammation. Front Immunol [Internet]. 2016 Apr 21 [cited 2020 Mar 4];7:145. Available from: http://journal.frontiersin.org/Article/10.3389/fimmu.2016.00145/abstract
60. Chen J, Xie J, Jiang Z, Wang B, Wang Y, Hu X. Shikonin and its analogs inhibit cancer cell glycolysis by targeting tumor pyruvate kinase-M2. Oncogene [Internet]. 2011 Oct 25 [cited 2019 May 28];30(42):4297–306. Available from:

http://www.nature.com/articles/onc2011137
61. Matsuhashi T, Hishiki T, Zhou H, Ono T, Kaneda R, Iso T, et al. Activation of pyruvate dehydrogenase by dichloroacetate has the potential to induce epigenetic remodeling in the heart. J Mol Cell Cardiol [Internet]. 2015 May [cited 2020 Mar 5];82:116–24. Available from: http://www.ncbi.nlm.nih.gov/pubmed/25744081
62. Tran Q, Lee H, Park J, Kim S-H, Park J. Targeting Cancer Metabolism - Revisiting the Warburg Effects. Toxicol Res [Internet]. 2016 Jul [cited 2020 Mar 5];32(3):177–93. Available from: http://www.ncbi.nlm.nih.gov/pubmed/27437085
63. Poff A, Koutnik AP, Egan KM, Sahebjam S, D'Agostino D, Kumar NB. Targeting the Warburg effect for cancer treatment: Ketogenic diets for management of glioma. Semin Cancer Biol [Internet]. 2019 Jun [cited 2020 Mar 3];56:135–48. Available from: http://www.ncbi.nlm.nih.gov/pubmed/29294371
64. Moussaieff A, Rouleau M, Kitsberg D, Cohen M, Levy G, Barasch D, et al. Glycolysis-Mediated Changes in Acetyl-CoA and Histone Acetylation Control the Early Differentiation of Embryonic Stem Cells. Cell Metab [Internet]. 2015 Mar 3 [cited 2018 Oct 25];21(3):392–402. Available from: http://www.ncbi.nlm.nih.gov/pubmed/25738455
65. Martínez-Reyes I, Chandel NS. Acetyl-CoA-directed gene transcription in cancer cells. Genes Dev [Internet]. 2018 Apr 1 [cited 2020 Mar 5];32(7–8):463–5. Available from: http://www.ncbi.nlm.nih.gov/pubmed/29692354
66. Zhang T, Kraus WL. SIRT1-dependent regulation of chromatin and transcription: linking NAD(+) metabolism and signaling to the control of cellular functions. Biochim Biophys Acta [Internet]. 2010 Aug [cited 2020 Mar 5];1804(8):1666–75. Available from: http://www.ncbi.nlm.nih.gov/pubmed/19879981
67. Xian Z-Y, Liu J-M, Chen Q-K, Chen H-Z, Ye C-J, Xue J, et al. Inhibition of LDHA suppresses tumor progression in prostate cancer. Tumour Biol [Internet]. 2015 Sep [cited 2019 May 28];36(10):8093–100. Available from: http://www.ncbi.nlm.nih.gov/pubmed/25983002
68. Ward PS, Thompson CB. Metabolic reprogramming: a cancer hallmark even warburg did not anticipate. Cancer Cell [Internet]. 2012 Mar 20 [cited 2019 Jun 28];21(3):297–308. Available from: http://www.ncbi.nlm.nih.gov/pubmed/22439925
69. Cantu D, Schaack J, Patel M. Oxidative inactivation of mitochondrial aconitase results in iron and H2O2-mediated neurotoxicity in rat primary mesencephalic cultures. PLoS One [Internet]. 2009 Sep 18 [cited 2020 Mar 6];4(9):e7095. Available from: http://www.ncbi.nlm.nih.gov/pubmed/19763183